

TECHNICAL UNIVERSITY OF CRETE

ELECTRONIC & COMPUTER ENGINEERING DEPARTMENT

ELECTRIC CIRCUITS & RENEWABLE ENERGY SOURCES LABORATORY



Isolated Electrical Power Systems Optimal Interconnections Planning

Emmanouil Loukarakis

Thesis submitted for the degree of Master of Science
in Electronic & Computer Engineering

Supervisory Committee

Prof. Georgios Stavrakakis (supervisor)
Prof. Kostantinos Kalaitzakis
Assistant Prof. Eftichios Koutroulis

Chania, Greece, March 2012

Abstract

The target of this work is the determination of the optimal solution in transmission expansion planning in the particular case of isolated systems involving dc interconnections. Therefore special attention is given to dc-links modeling aspects for steady state analysis, as well as security constraints relevant to small sized systems operation. Therein lies the first contribution of this work, namely in the incorporation of operating reserve related considerations and simplified dc-links models in isolated systems planning. The proposed method combines a Monte-Carlo simulation which enables the probabilistic assessment of power system operation, with an adaptive enumeration technique which recurrently determines and evaluates investment scenarios of interest, based on suitable probabilistic indices. This constitutes the second contribution of this work, as a map of all meaningful solutions to the planning problem may be generated, which in turn allows not only the determination of the optimal solution, but also the evaluation of the effects of over- or under-investment in certain parts of the grid.

Περίληψη

Αντικείμενο της παρούσας εργασίας είναι η μελέτη διασυνδέσεων συστημάτων ενέργειας εστιάζοντας όχι τόσο στο σχεδιασμό των επιμέρους κατασκευαστικών τους στοιχείων, αλλά κύρια στην αξιολόγηση πιθανών διασυνδέσεων από την πλευρά σχεδιασμού του συστήματος ενέργειας. Για το σκοπό αυτό αναπτύσσεται μια μέθοδος για την εκτίμηση της αξίας τέτοιων επενδύσεων και την εύρεση της βέλτιστης λύσης στο εν λόγω πρόβλημα. Ιδιαίτερη έμφαση δίνεται στην περίπτωση απομονωμένων συστημάτων και κατά συνέπεια σε θέματα προσομοίωσης dc διασυνδέσεων και περιορισμών ασφάλειας σχετικών με την λειτουργία "μικρού" μεγέθους συστημάτων ενέργειας. Η προτεινόμενη μέθοδος μπορεί εύκολα να επεκταθεί για να καλύψει ιδιαιτερότητες που παρουσιάζει η λειτουργία των απελευθερωμένων αγορών ενέργειας, καθώς και αβεβαιότητες που μπορεί να παρουσιάζονται κατά τη σχεδίαση ανάπτυξης του συστήματος.

Η εκτίμηση της αξίας κάθε πιθανής επένδυσης βασίζεται στην πιθανοτική ανάλυση της λειτουργίας του συστήματος. Για το σκοπό αυτό χρησιμοποιείται μία μέθοδος Monte-Carlo η οποία επιτρέπει την δημιουργία πιθανών καταστάσεων λειτουργίας. Η επίλυση του προβλήματος βέλτιστης ροής φορτίου που αντιστοιχεί σε κάθε μία από αυτές και ο συνδυασμός των αποτελεσμάτων οδηγεί στον υπολογισμό δεικτών αξιολόγησης της επένδυσης. Η προσέγγιση αυτή επιτρέπει να ληφθούν υπόψη οι διακυμάνσεις στο κόστος παραγωγής ενέργειας στο σύστημα τόσο λόγω της μεταβολής των φορτίων κατά τη διάρκεια της ημέρας, όσο και λόγω των αυξομειώσεων της διαθέσιμης παραγωγής από ανανεώσιμες πηγές ενέργειας ή της διαθεσιμότητας των συμβατικών μονάδων.

Η διερεύνηση της βέλτιστης λύσης στο πρόβλημα της διασύνδεσης βασίζεται σε μία μέθοδο προσαρμοστικής απαρίθμησης. Η μέθοδος αυτή βασίζεται στην υπόθεση ότι η ανάγκη για επένδυση σε οποιοδήποτε τμήμα του συστήματος ενέργειας μπορεί να περιγραφεί με κατάλληλα επιλεγμένους πιθανοτικούς δείκτες. Με βάση τους δείκτες αυτούς μπορούν να βρεθούν και να αξιολογηθούν όλα τα σενάρια που μπορεί να παρουσιάζουν επενδυτικό ενδιαφέρον. Παράλληλα μπορεί να καταστρωθεί ένας χάρτης / δέντρο επενδύσεων που επιτρέπει την εκτίμηση των επιπτώσεων επιλογής λύσεων διαφορετικών από τη θεωρούμενη βέλτιστη.

Ως ενδεικτικό παράδειγμα εφαρμογής της παραπάνω μεθόδου χρησιμοποιείται μια πιθανή διασύνδεση του συστήματος της Κρήτης με το ηπειρωτικό σύστημα. Τα παρουσιαζόμενα αποτελέσματα υποδεικνύουν την επίδραση της διασύνδεσης στη λειτουργία του συστήματος, καθώς και τις σημαντικές επιπτώσεις στα τελικά οφέλη της επένδυσης, που μπορεί να έχουν περιορισμοί ασφαλούς λειτουργίας όπως για παράδειγμα η απαίτηση για τήρηση εφεδρείας.

Acknowledgements

The author would like to express his gratitude and appreciation to his supervisor Prof. Georgios Stavrakakis for his advice, encouragement and multifaceted support, and will remain deeply indebted to him. The author would also like to thank the two other members of his supervisory committee, Prof. Konstantinos Kalaitzakis and Prof. Eftichios Koutroulis, for their guidance and excellent cooperation. Finally the author expresses his thanks to his family for their enduring support and encouragement during his studies.

Contents

Introduction	1
1.1 Problem Definition.....	1
1.2 Interconnecting Power Systems	1
1.3 Literature Review.....	2
1.4 Thesis Outline	3
HVDC Interconnections	5
2.1 Introduction.....	5
2.2 Current Source Converters	5
2.2.1 Line Commutated Thyristor Converter 6-Pulse Bridge.....	5
2.2.2 Line Commutated Thyristor Converter 12-Pulse Bridge.....	8
2.3 Voltage Source Converters	9
2.4 Capacitor Commutated Converters	11
2.5 Interconnection Configurations	12
2.6 Modeling, Operation and Control.....	12
2.6.1 Line Commutated Current Source Converters.....	12
2.6.2 Self Commutated Voltage Source Converters.....	13
2.7 DC Link Design Aspects.....	14
2.7.1 Converter Components	14
2.7.2 Underground / Submarine Cables.....	14
2.7.3 Overhead Lines and Earth Electrodes.....	15
2.8 Interaction Between AC and DC Systems.....	16
Power System Probabilistic Assessment	19
3.1 Introduction.....	19
3.2 Monte Carlo Simulation Approaches	19
3.3 State Samples Generation	20
3.3.1 Inverse Transform Method	20
3.3.2 Correlated Random Numbers Generation.....	20
3.3.3 Power System Components Modeling	21
3.4 Convergence Conditions.....	23

Power System Steady State Analysis	25
4.1 Introduction	25
4.2 Power Flow Equations	25
4.3 Optimal Power Flow Formulation	26
4.3.1 AC Transmission Losses Approximation	26
4.3.2 DC Interconnection Modeling	27
4.4 Security Constraints Consideration	27
4.4.1 System Reserve Level	28
4.4.2 Reserve Cost and Distribution	30
4.5 Optimal Power Flow Equations Summary	31
4.6 Interior Point Optimization Algorithm	32
Power System Planning	35
5.1 Introduction	35
5.2 Investment Evaluation Criteria	35
5.2.1 Economic Evaluation	35
5.2.2 Reliability Evaluation	36
5.2.3 Investment Costs	36
5.3 Short Term (Static) Problem	37
5.4 Indicative Results	38
5.4.1 Test System	38
5.4.2 Interconnection Effects Assessment	39
5.4.3 Adaptive Enumeration Method Results	40
5.5 Long Term (Dynamic) Problem	41
Conclusions	43
6.1 Conclusions	43
6.2 Future Work	43
References	45

Introduction

1.1 Problem Definition

The subject of this work is power systems interconnections, focusing not so much on the various design aspects of their individual components, but on the evaluation of a potential interconnection from a power system planning perspective. For that purpose a framework for the worth assessment of a potential investment has to be established, and a method for selection of the optimal expansion plan among those available has to be defined. This bears many similarities to the traditional transmission expansion problem. The location, type, and time of the investment have to be determined, based on a combination of economic and reliability criteria. However, due to the impact that an interconnection might have on system operation, security considerations not commonly accounted for in system planning studies, have also to be taken into account.

Particular attention in this work is given to the interconnection of isolated power systems. In the general case these involve small or medium sized networks covering the needs of an island. These interconnections are most often of dc type, and use submarine cables. Furthermore, the most prominent security consideration in such systems has to do with the required operating reserve. As a result the focus is on these three points. However this does not compromise the methods or results presented, as with few modifications, any type of relevant problem (e.g. involving ac interconnections, additional security considerations etc.) may be effectively solved.

1.2 Interconnecting Power Systems

Both ac and dc links are viable options for power system interconnections. The use of one or the other technology depends on the usual combination of economic and technical considerations. As far as costs are concerned for small distances ac is always preferable, as dc additionally requires converters. There is however a breakeven distance of about 450 km for overhead lines and 50-100 km for cables [1], over which dc is preferable. The reason is that costs associated with transmission losses and installation of shunt capacitors (to compensate the reactive character of ac lines) result in a much higher ac-link total cost than that of a dc-link. Overhead dc lines typically involve simpler constructions and smaller right of way. The skin effect, dielectric and eddy current losses and the resulting aging of the insulation material (in cables) are issues encountered only in ac transmission.

Interconnection of independent systems with ac links requires careful consideration of stability and control issues. Load flow in ac grids depends on the angle difference of bus voltage vectors which is controlled by the relatively slow systems of conventional generators. Thus, dynamic voltage stability issues have to be accounted for, and controls should be such that inter-area oscillations are avoided. For a reliable interconnection more than one ac-links will generally be required. On the contrary a dc-link offers fast power control capability and inherently features the control capability to damp power oscillations in each connected system. Furthermore faults causing voltage depression do not transmit across the dc-link. Depending on the dc-link type, operation is also possible under any voltage or frequency conditions, while voltage amplitude and reactive power may also be controlled. Thus, stability issues of a similar scope to those raised with ac transmission, are practically negated. Practices regarding reliability and security may be determined separately for each system, and largely independently of the dc-link.

For all intents and purposes ac interconnections can be treated simply as additional ac lines. Dc links however are rather more complex and overall require a different treatment in power system

simulations of any type. For these reasons, a significant part of this work focuses solely on dc interconnections.

1.3 Literature Review

The literature on power system planning, and particularly transmission expansion planning, is rather extensive. A review of relevant methods may be found in [2], according to which the various methods may be classified either as those based on mathematical optimization models (linear or non-linear programming, dynamic programming, mixed integer programming etc.), or as those using various heuristic rules (i.e. improving an initial plan through a step by step procedure based on logical rules, empirical criteria or sensitivities). The latter category also includes various random search methods such as genetic algorithms, particle swarm optimization etc. An additional factor differentiating various methods is the way of treatment of the planning horizon, i.e. static or dynamic planning. More recent publications in this area of research do not fall outside of these categories, though additional complexities have been added due to the liberalization of electricity markets.

Given the wide range of operating states a power system might find itself in, and the fact that reliability also is a factor affecting investments in transmission, several papers have taken a probabilistic approach to planning. In [3] reliability constraints are added to the relevant optimization problem, using analytical methods to calculate the required reliability indices. In [4] a Monte-Carlo approach is used to estimate various market related indices, and price profile flatness is introduced as a criterion for the determination of where new transmission lines should be built. An interesting backward heuristic approach is taken in [5] where an initial system evaluation is conducted with all possible investments included. Then, based on a least performance index, the investments are removed one by one until some type of violation comes up. A disadvantage in this approach however is that candidate investments have all to be known at the start of solution.

The typical transmission expansion problem is extended in [6] through the addition of N-1 contingency and CO_2 emission constraints. In [7] a stochastic programming approach is taken to solve a vulnerability constrained transmission expansion problem. Similarly in [8] transmission system outages are accounted for, and the optimal solution is selected based also on the risk associated with the vulnerability of the network. A method for including N -a security criteria is proposed in [9], using a branch and bound based integer programming approach. Reference [10] focuses on congestion driven transmission expansion, using Bender's decomposition techniques to solve the discrete multi-period problem.

Uncertainties related to future generation expansion and different market rules are considered in [11]. Several transmission expansion scenarios are generated, a Monte-Carlo process is used to access the power system operation in each scenario, and an adaptation cost is estimated for the various uncertainties. The optimal expansion plan is selected based on its flexibility (i.e. minimum adaptation cost to different scenarios). Also in [12] various uncertainties, including those related to market players behavior, are taken into account by considering a set of scenarios. Three different objectives are considered over that set: minimization of social welfare, minimization of investment costs and regret (i.e. social welfare increase compared to the minimum possible) related to any arbitrary expansion plan. Genetic algorithms are utilized to find pareto optimal solutions. In [13] uncertainties in demand growth and system components availability are covered through scenario generation by a Monte-Carlo process. Interactions between the independent system operator and various generation and transmission companies are also simulated.

While the above mentioned publications cover a small percentage of published work in this area, they are indicative of the general issues related to the formulation and solution of the problem itself. Namely these deal with inclusion of security constraints, uncertainties consideration, market players behavior modeling and probabilistic evaluation of system operation performance. In this work a method is proposed for power system planning, generally applicable independently of the problem formulation. It particularly focuses on the first and last of the aforementioned issues, though it is easily extensible and may also cover the remaining two. Its main contributions relate to: 1) the establishment of a framework for power system investments evaluation based on an map generated through an adaptive enumeration process, and 2) treatment of particular issues in the dc interconnection planning in relatively small sized systems.

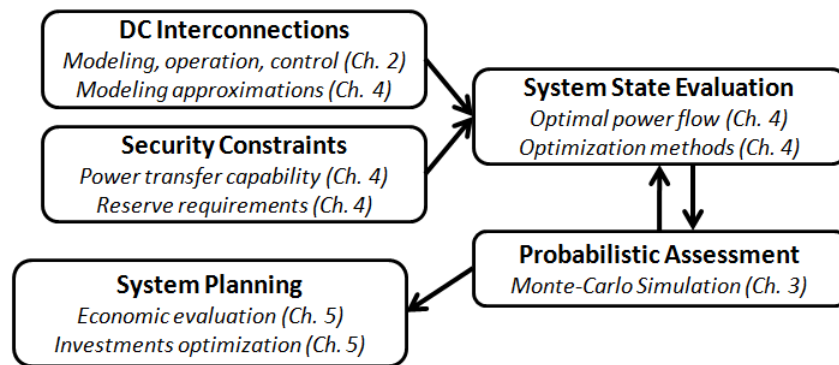


Fig. 1.1. Thesis structure, presented concepts and chapters association..

1.4 Thesis Outline

This thesis is organized in five basic chapters. Since the focus of this work is on power system planning, detailed modeling and operation characteristics assessment is not of primary importance here. Nevertheless the following chapter focuses in exactly these subjects, and serve as a basis for the justification of the simplified models which are finally used. The final four chapters present the key components and indicative results of the proposed method for optimal interconnection sizing. More specifically:

Chapter 2 gives an introduction in ac / dc conversion and describes the most commonly used power electronics converters used in high voltage dc interconnections. Based on these models elements related to modeling and control of a full dc interconnection are described. A brief introduction to design elements of cable based dc-links is given, and basic issues related to their interaction with ac systems are discussed.

Chapter 3 presents the basic elements of Monte-Carlo methods used for the probabilistic assessment of power system operation.

Chapter 4 describes the formulation of the optimal power flow method, used for the determination of system costs. Simplified models for dc-link modeling are also presented.

Chapter 5 completes the presentation of the planning method and concludes with some indicative results, concerning a potential interconnection between the isolated island system of Crete with mainland Greece.

Chapter 6 summarizes the results of this work and discusses potential improvements and extensions for the presented method.

The above concepts are summarized in Fig. 1.1, where the relations between them are also visualized. Essentially chapters 2 and 4 focus in single operating state and single investment assessment. Chapter 3 extends the analysis to multiple state, single investment evaluation. Finally chapter 5 covers multiple states, multiple investments assessment.

HVDC Interconnections

2.1 Introduction

This chapter serves as an introduction to HVDC interconnections. The basis of any such interconnection is the ac/dc converter. In the following sections, the basic topologies used for ac to dc conversion (and vice versa) are presented. There are essentially two types of three-phase converters [14]: Current Source Converters (CSC) and Voltage Source Converters (VSC), typically utilizing thyristors (SCR) and integrated gate bipolar transistors (IGBT) respectively. The basic operating principles of these two topologies will be discussed in detail in the following subsections, based on simulations in Matlab/Simulink. Basic relations between ac and dc quantities are established that will form the basis of interconnections modeling. A brief reference to capacitor commutated converters is also included. Typical HVDC interconnection configurations are presented along with basic models suitable for the representation of dc-links in power flow studies. Their operation and control principles are briefly analyzed. All presented converters serve both as rectifiers and as inverters. Design and operation factors affecting costs and reliability are also discussed. Special attention is given in submarine interconnections.

2.2 Current Source Converters

Current source converters utilizing thyristors are the classic topology used in dc interconnections. The basic topologies used are the 6-pulse bridge converter, and most importantly the 12-pulse bridge converter. These variants will be described in the following subsections.

2.2.1 Line Commutated Thyristor Converter 6-Pulse Bridge

The equivalent circuit in its simplest form may be seen in Fig. 2.1. The converter is controlled by modifying the delay α of the thyristor valve ignition pulses. The analysis that follows [15,14] assumes that:

- Converter valves are ideal switches, that is they have no resistance when conducting and infinite resistance when not conducting.
- The ac system is perfectly balanced, and commutation inductances L_k are symmetrical.
- The dc current is ripple free, which implies that a large smoothing inductance is on the dc side.

First the case where $L_k = 0$ is considered. At any time two valves conduct depending on the ac voltages

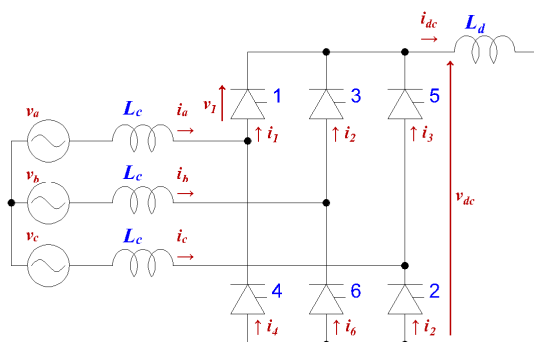


Fig. 2.1. Three phase current source converter basic topology (6-pulse converter).

values. For example without ignition delay the thyristor valves 1 and 2 conduct while v_{ab} , v_{ac} and v_{bc} are all positive. Of course a pulse has to be given at the gate of each thyristor at the appropriate moment. Depending on which valves conduct, the corresponding phase to phase voltage is seen on the dc side, as illustrated in Fig. 2.3. As can be observed, within a single period (0.02 s) the dc voltage has six pulsations (hence the name "6-pulse bridge circuit"). The average dc voltage may be estimated by averaging the phase to phase voltage over a 60° period:

$$V_{dc}^0 = \frac{3\sqrt{2}}{\pi} V_{ab} \int_{\pi/3}^{2\pi/3} \sin(x) dx = \frac{3\sqrt{6}}{\pi} V_a \approx 2.34V_a \tag{2.1}$$

Where V_a the rms value of v_a . With ignition delay the voltage changes as can be seen on Fig. 2.6 and may be estimated by the relation:

$$V_{dc} = \frac{3\sqrt{2}}{\pi} V_{ab} \int_{\pi/3+\alpha}^{2\pi/3+\alpha} \sin(x) dx = \frac{3\sqrt{6}}{\pi} V_a \cos(\alpha) \approx V_{dc}^0 \cos(\alpha) \tag{2.2}$$

For values of α larger than 90° then v_{dc} reverses (Fig. 2.8, Fig. 2.9) and power flows from the converter to the grid. Inverter operation presupposes the presence of a dc power source. The rms value of the ac current may be estimated by Fourier analysis of the current waveform:

$$I_a = \frac{2}{\pi\sqrt{2}} \int_{-\pi/3}^{\pi/3} I_{dc} \cos(x) dx \approx 0.78I_{dc} \tag{2.3}$$

If converter losses are neglected then the ac active power must be equal to the dc power. Thus:

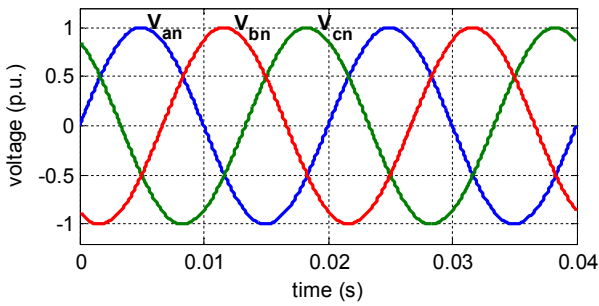


Fig. 2.2. Phase to neutral voltages.

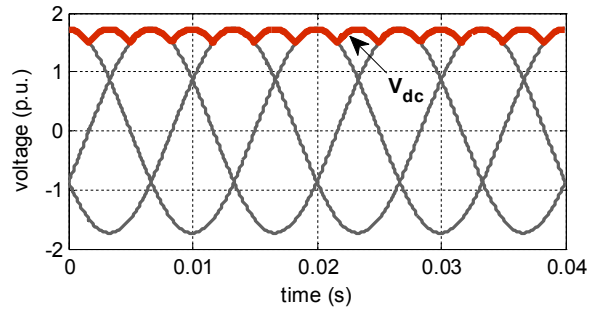


Fig. 2.3. Phase to phase voltages and v_{dc} ($\alpha = 0^\circ$).

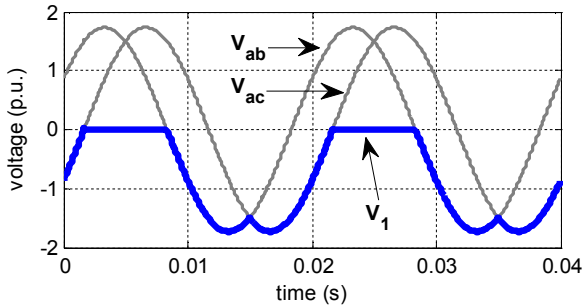


Fig. 2.4. Voltage on thyristor valve 1 ($\alpha = 0^\circ$).

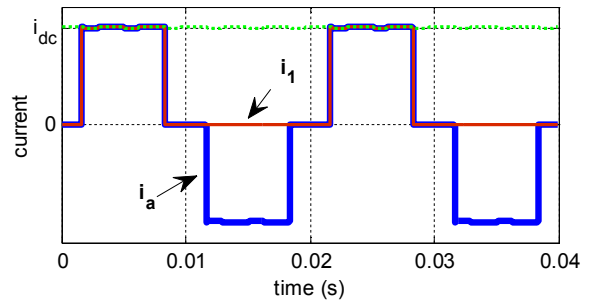


Fig. 2.5. Converter currents ($\alpha = 0^\circ$).

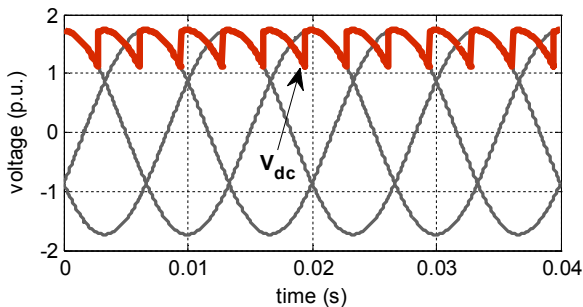


Fig. 2.6. Phase to phase voltages and v_{dc} ($\alpha = 20^\circ$).

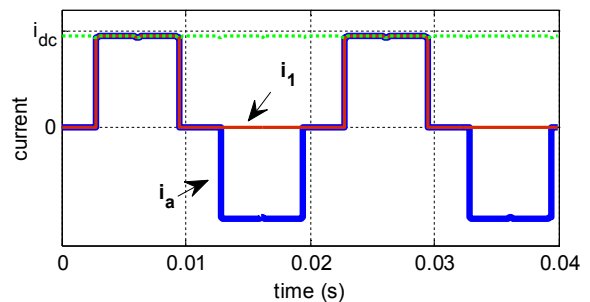


Fig. 2.7. Converter currents ($\alpha = 20^\circ$).

$$3V_a I_a \cos \varphi = V_{dc} I_{dc} \quad (2.4)$$

Substituting for I_a and V_{dc} based on (2.1) to (2.3) then:

$$\cos \varphi = \cos \alpha \quad (2.5)$$

This relation implies that the reactive power consumed by the converter depends on the ignition delay α . Furthermore, given that α theoretically ranges from 0° to 180° , reactive power is always absorbed by the converter. Typically some sort of compensation (e.g. using capacitor banks) has to be provided during the dc-link's operation. For power system simulation purposes it may be assumed that the converter reactive power is equal to the reactive power of the first current harmonic. Finally it should be noted that for inverter operation the symbol γ is typically used instead of α .

Let us now consider the case where $L_k > 0$. Due to this impedance the current in each phase cannot change instantly. The transfer of current from one phase to another requires a period of time called commutation time. During this time three thyristors conduct simultaneously. The corresponding angle is the commutation or overlap angle μ , and its value ranges typically from 15° to 20° . Values of μ larger than 60° as can be expected result in abnormal operation. The effect of L_k can be seen on Fig. 2.10 and Fig. 2.11. Considering the commutation from phase a to phase b (valve 1 to valve 3) with valve 2 conducting then the following relation stands:

$$I_{dc} = i_1 + i_3 \Rightarrow \frac{di_1}{dt} = -\frac{di_3}{dt} \quad (2.6)$$

Consequently

$$v_b - v_a = L_c \frac{di_3}{dt} - L_c \frac{di_1}{dt} = 2L_c \frac{di_3}{dt} \quad (2.7)$$

Thus the dc voltage during this commutation is:

$$v_{dc} = v_b - L_c \frac{di_3}{dt} - v_c = \frac{v_b + v_a}{2} - v_c \quad (2.8)$$

This results in an average reduction of the expected dc voltage that may be estimated as follows:

$$\Delta V_{dc} = \frac{3\sqrt{6}V_a}{2\pi} \int_a^\delta \sin(x) dx = \frac{3\sqrt{6}V_a}{2\pi} (\cos(\alpha) - \cos(\delta)) = \frac{V_{dc}^0}{2} (\cos(\alpha) - \cos(\delta)) \quad (2.9)$$

where $\delta = \alpha + \mu$. Integrating (2.7) and taking into account that $i_3(\delta) = I_{dc}$, results in the following relation for the dc current:

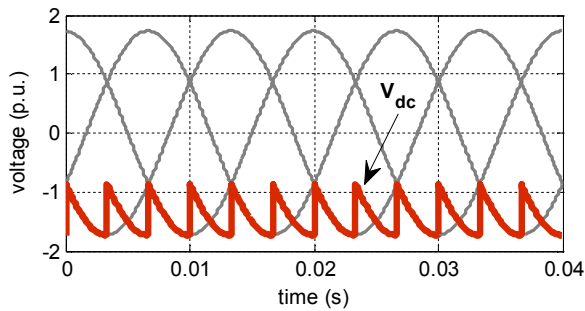


Fig. 2.8. Phase to phase voltages and v_{dc} ($\alpha = 150^\circ$).

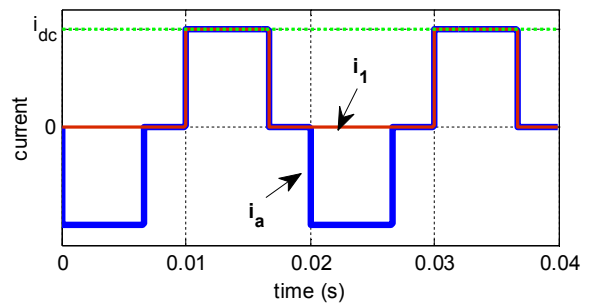


Fig. 2.9. Converter currents ($\alpha = 150^\circ$).

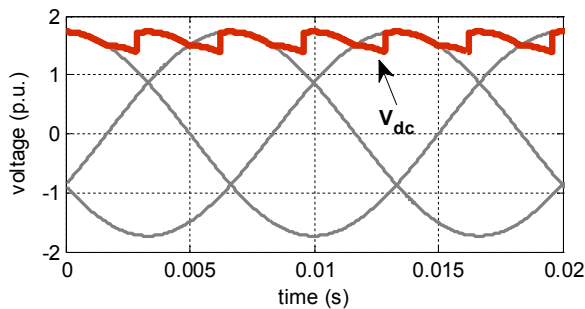


Fig. 2.10. Effect of L_k on voltage ($\alpha = 0^\circ$).

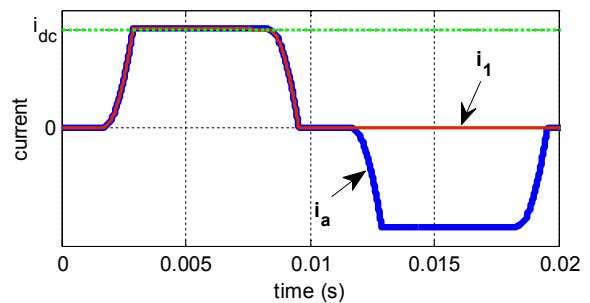


Fig. 2.11. Effect of L_k on currents ($\alpha = 0^\circ$).

$$I_{dc} = \frac{\sqrt{6}}{2\omega L_c} V_a (\cos(\alpha) - \cos(\delta)) \tag{2.10}$$

The above equations are valid for the whole operating range of the converter. It should be noted that this effect of L_k reduces the possible range of values for α . Additionally, due to the rounding off of the otherwise rectangular current pulses edges, harmonics are slightly reduced too.

Summing up the above, equations relating ac with dc quantities may be derived. Based on equations (2.2) and (2.9) the following relation stands for the voltage:

$$V_{dc} = \frac{3\sqrt{6}}{\pi} \frac{\cos(\alpha) + \cos(\delta)}{2} V_a \tag{2.11}$$

Similarly, combining equations (2.4) and (2.11) the following relation is derived for the current:

$$I_a \cos(\varphi) = \frac{\sqrt{6}}{\pi} I_{dc} \frac{\cos(\alpha) + \cos(\delta)}{2} \tag{2.12}$$

The above relations may be simplified by assuming that:

$$\cos(\varphi) \approx \frac{\cos(\alpha) + \cos(\delta)}{2} \tag{2.13}$$

This assumption typically gives an error smaller than 4% for typical values of μ [15].

2.2.2 Line Commutated Thyristor Converter 12-Pulse Bridge

In case the voltage or current rating is so high that a single thyristor does not suffice, multiple thyristors may be connected in series or in parallel. However this presents the difficult problem of matching the devices in static and switching conditions [1]. Thus in practice rather than single thyristors, whole converters are used in series or parallel operation using phase-shifting transformers. The most common such configuration is the so called 12-pulse bridge illustrated in Fig. 2.12. A significant benefit of this particular topology is the reduction of harmonics as described in [15]. In cases where more than two bridges are required higher pulse numbers are possible that allow further reduction of harmonics. However, due to the increased complexity, the use of multiple 12-pulse converters is more practical. Thus this configuration is almost exclusively used for modern HVDC links[16].

In the general case, assuming k converters are connected in series, with a transformer ratio t , the average dc current is given by:

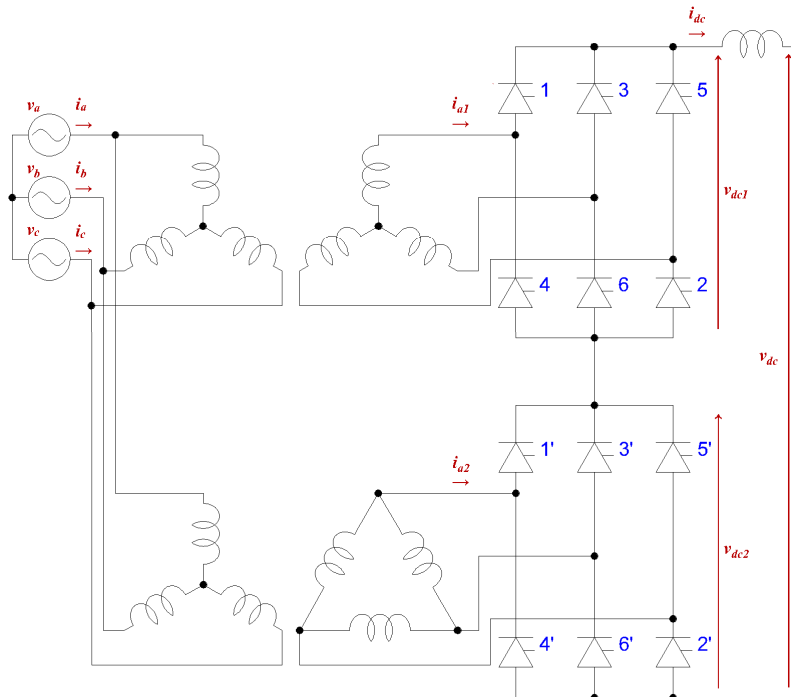


Fig. 2.12. Three phase current source 12-pulse converter.

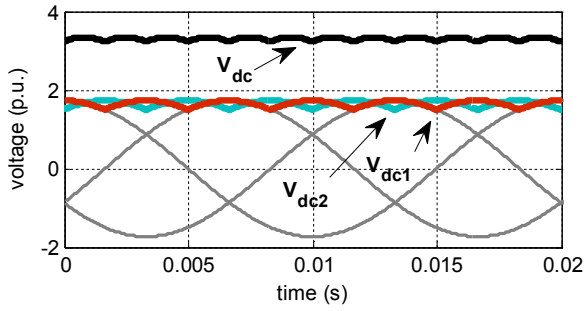


Fig. 2.13. Phase to phase and dc voltages for the 12-pulse bridge converter ($a = 0^\circ$).

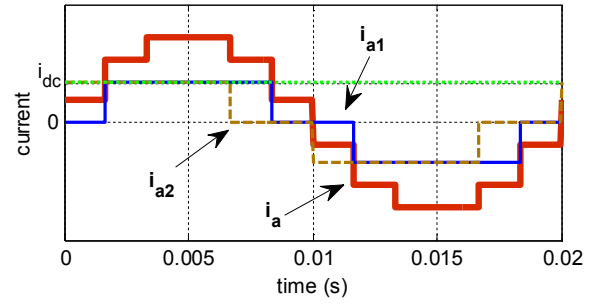


Fig. 2.14. Currents for the 12-pulse bridge converter ($a = 0^\circ$).

$$I_{dc} = \frac{\sqrt{6}}{2\omega L_c} t V_a (\cos(a) - \cos(\delta)) \quad (2.14)$$

and the dc voltage:

$$V_{dc} = \frac{3\sqrt{6}}{\pi} \frac{\cos(a) + \cos(\delta)}{2} k t V_a = \frac{3\sqrt{6}}{\pi} k t V_a \cos(a) - \frac{3\omega L_c}{\pi} k I_{dc} = V_{dc}^0 \cos(a) - R_{dc} I_{dc} \quad (2.15)$$

Also based on (2.4) the following relation stands:

$$I_a \cos(\varphi) = \frac{\sqrt{6}}{\pi} k t I_{dc} \frac{\cos(a) + \cos(\delta)}{2} \quad (2.16)$$

In the specific case of the 12-pulse bridge the expected current and voltage waveforms, assuming a transformer ratio of 1, may be seen on Fig. 2.13 and Fig. 2.14. The dc voltage is the sum of the voltage outputs of the two bridges. Voltage pulses on the dc side are doubled however due to the 30° phase shift, which is introduced by the Y- Δ connection of the transformer.

2.3 Voltage Source Converters

The essential difference between VSC and CSC converters is that the former use self-commutating switches rather than line-commutating. In the analysis that follows the assumptions that were made in the previous sections still stand. However instead of an infinite inductance, an infinite capacitance is assumed on the dc side. A commonly used VSC converter may be seen on Fig. 2.15. The IGBTs may be replaced by other self commutating devices such as GTOs. While thyristors may be turned on only once during each cycle no such restriction applies here. Each pair of IGBTs connected in series constitutes a single switch, which depending on its state, connects the respective ac phase voltage either to the high or low dc voltage. Thus there are a total of 3 switches, one for each phase, giving 8 possible states for the ac voltage at the converter terminals. Typically, a pulse width modulation (PWM)

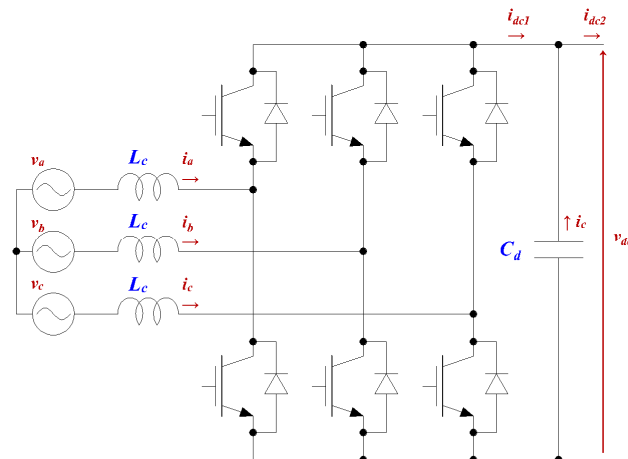


Fig. 2.15. Three phase voltage source igbt converter.

method is used to control the switches. The type of PWM determines the relation between the dc and ac voltage.

There is a wide variety of PWM methods including sinusoidal, harmonic elimination, minimum ripple current, space vector etc [1]. A review of several PWM methods may be found in [17]. Essentially such a method has to balance three things: generated harmonics, conversion losses and dc-link voltage utilization. This shall be illustrated through a brief analysis of the simple and most commonly used sinusoidal PWM. For the transistors corresponding to each phase pulses are generated by comparing a sine-wave with a triangular signal as illustrated in Fig. 2.16 and Fig. 2.17. The fundamental frequency of the generated voltage is equal to the sine-wave frequency. In addition changing the sinusoidal carrier phase, will in turn change the phase of the ac voltage. In the converter operation two quantities are of interest. First, the frequency modulation factor, which is defined as the ratio of the modulation frequency to the output frequency:

$$m_f = f_p / f \tag{2.17}$$

Second, the amplitude modulation factor, which is defined as the ratio of the two waves amplitude:

$$m_a = A_w / A_{sin} \tag{2.18}$$

The amplitude modulation factor determines the rms of the generated voltage fundamental harmonic, that is [18]:

$$V_{a(0)} = \frac{1}{2\sqrt{2}} m_a V_{dc} \tag{2.19}$$

Typically $m_a \leq 1$. However higher voltage might be achieved through overmodulation ($m_a > 1$) at the cost of increased harmonic content. The modulation frequency factor mostly affects the generated harmonics. Generally m_f should be selected to be an odd multiple of 3, as this effectively cancels several harmonics. In addition given that harmonics appear as bands around multiples of f_p , and high order harmonics are easier to suppress, it is desirable to have a high m_f value. Of course this in turn increases switching losses. The aforementioned effects of the two modulation factors may be seen in Fig. 2.18 and Fig. 2.19.

In order to better clarify the operation and control of this particular inverter, a transition to a d-q

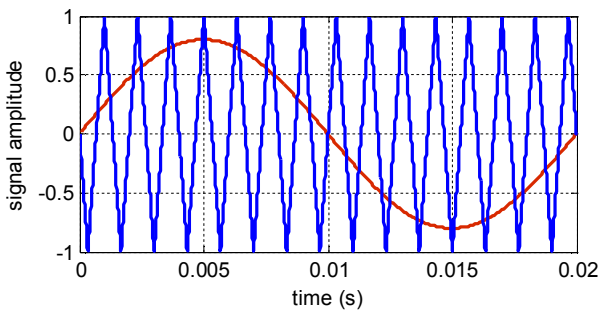


Fig. 2.16. Compared signals for phase a pulse generation with $m_a = 0.8$ and $m_f = 15$.

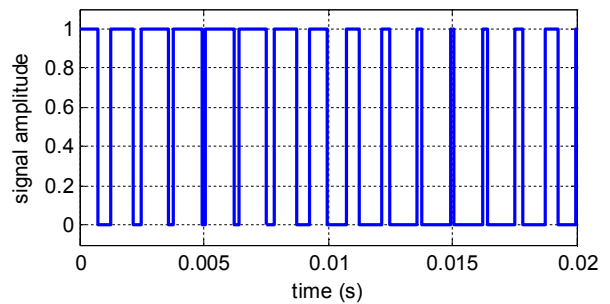


Fig. 2.17. Generated pulses for upper IGBT corresponding to phase a. The pulses for the other transistor are complementary to those shown above.

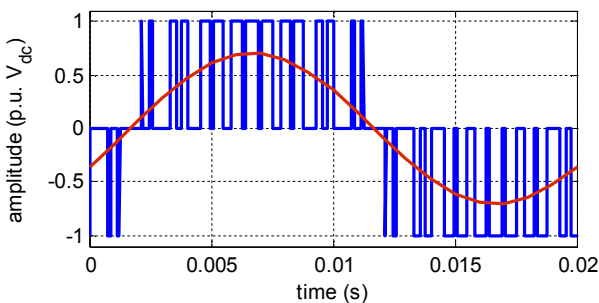


Fig. 2.18. Converter ac voltage output between phase a and b and corresponding 1st harmonic.

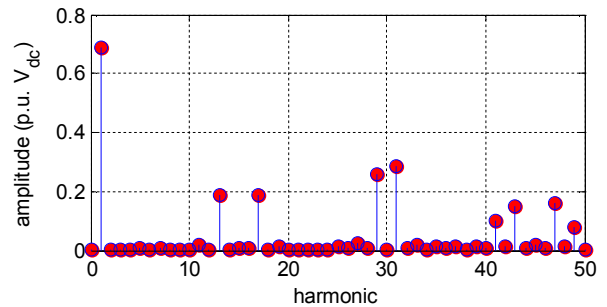


Fig. 2.19. Voltage harmonics.

system is necessary. For that purpose the following transformation is used [15]:

$$\mathbf{v} = \frac{2}{3}(v_a + av_b + a^2v_c)e^{-j\omega t} \quad (2.20)$$

where ω is the rotational speed of the d-q reference frame. The voltage vector may be further analyzed as $\mathbf{v} = v_d + jv_q$. The d-q voltage vector is directly related to the voltage phasor. Specifically if only the fundamental harmonic is considered in the above equation, and \mathbf{V} is the phase to ground voltage phasor then:

$$\mathbf{V} = \frac{\|\mathbf{v}\|}{\sqrt{2}}e^{j\angle v} \quad (2.21)$$

The same relations apply to currents. Finally, applying the transformation to the voltage equations for the ac side:

$$\mathbf{v} - \mathbf{v}_c = j\omega L_c \mathbf{i} + L_c \frac{d}{dt} \mathbf{i} \quad (2.22)$$

where \mathbf{v}_c the converter ac voltage. Assuming steady state operation, and that the selected d-q system is oriented to the grid voltage then the above equation may be rewritten as:

$$\begin{aligned} v_d - v_{cd} - \omega L_c i_q &= 0 \\ -v_{cq} + \omega L_c i_d &= 0 \end{aligned} \quad (2.23)$$

The power transmitted to the grid is then:

$$S = \frac{2}{3} \mathbf{v} \mathbf{i}^* = \frac{2}{3} v_d i_d + \frac{2}{3} j v_q i_q \quad (2.24)$$

This implies that active and reactive power to the grid may be controlled through the d and q current components respectively. In turn i_d and i_q may be controlled by v_{cq} and v_{cd} respectively. This requires the provision of a specific voltage vector from the converter, which is exactly what the PWM methods make possible. Assuming lossless conversion for the dc currents the following relation is valid:

$$v_{dc} i_{dc1} = \text{Re} \left[\frac{2}{3} \mathbf{v}_c \mathbf{i}^* \right] = \frac{2}{3} (v_{cd} i_d + v_{cq} i_q) \quad (2.25)$$

The above equations fully describe the converter model in steady state. Equation (2.19) can be expected to vary with different PWM schemes.

2.4 Capacitor Commutated Converters

Another type of converter topology utilized in dc-links, though not as commonly as the previously described types, is the capacitor commutated converter (CCC). As can be seen in Fig. 2.20 it is similar to the CSC converter of Fig. 2.1 with the addition of capacitors before the thyristors. This effectively changes the commutation process in the system. As a result the range of possible commutation angles increases. The ability to use low commutation angle values implies that reactive power consumption may be reduced and thus achieve an improved power factor. In addition, the maximum active power transfer capability is also improved. Furthermore, in case of voltage drops it behaves more favorably than standard CSC and the probability of commutation failures is decreased. Consequently it is more suitable in case of weak ac systems where voltage variations may be expected often. A similar converter is the so called controller series capacitor converter (CSCC) where a series capacitor is placed between the grid and the dc-link transformer. A more detailed analysis of these converter topologies may be found in [1].

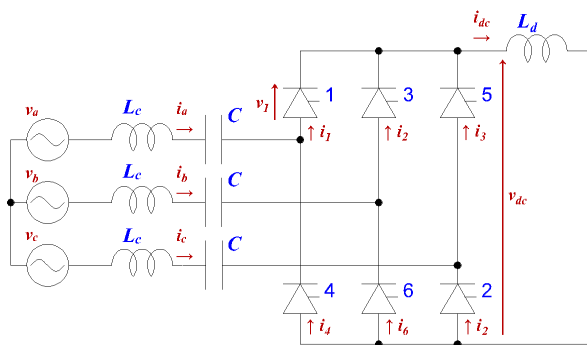


Fig. 2.20. Three phase capacitor commutated converter basic topology (6-pulse converter).

2.5 Interconnection Configurations

Point to point HVDC links may be classified in three categories [14]:

Monopolar links: Its basic configuration may be seen on Fig. 2.21. One conductor is used, usually of negative polarity. Earth or water is used as a return path. However a metallic return is required in case of high earth resistivity or interference with underground / submarine installations. Commonly the monopolar links are constructed as a first stage of a bipolar link.

Bipolar links: This is the most common interconnection type. As can be seen on Fig. 2.22 each terminal has two converters in series. Normally the dc-link is operated in such a way that the current return through the earth is zero. However each pole can be operated independently from the other. Thus in case one of the poles is isolated due to a fault, the other can continue operation and carry half the rated power or more depending on its overload capabilities. A third conductor may be added if necessary for the return.

Homopolar links: This type of dc-link, as can be seen on Fig. 2.23, uses as a return path the ground. The return current is equal to the current of the two metallic conductors. Because this kind of operation is undesirable this interconnection type is not generally used. It potentially offers the advantage of reduced insulation costs, and in addition in case of single conductor failure the full converter may still be used with relative ease compared to the bipolar links case. Still the disadvantages of earth return usually outweigh these benefits.

Apart from the aforementioned configurations there are also multi-terminal HVDC links, where the dc system is connected to more than two points of the ac network. Further information may be found in [16].

2.6 Modeling, Operation and Control

In this section models are presented that describe various dc-link types. It should be noted that the models are oriented towards steady state analysis. While the basic operation and control concepts will be discussed, a detailed control systems analysis is outside the scope of this work.

2.6.1 Line Commutated Current Source Converters

This converter type is usually represented by the 12-pulse thyristor bridge. A simplified schematic of this converter may be seen on Fig. 2.24 for a monopolar dc-link. The two basic assumptions are that the dc current is ripple free, and that harmonics are filtered effectively and do not propagate into the ac system. The equations that describe the dc-link, based on the relations presented in the previous chapter, are for the rectifier:



Fig. 2.21. Monopolar dc-link configuration.

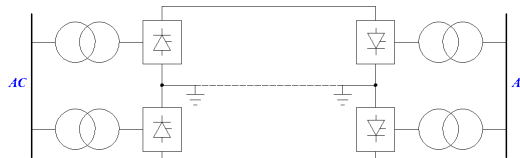


Fig. 2.22. Bipolar dc-link configuration.

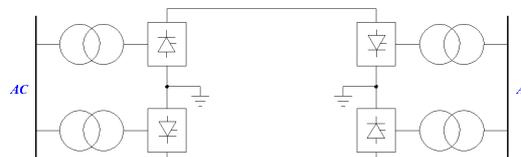


Fig. 2.23. Homopolar dc-link configuration.

$$V_R = \frac{3\sqrt{6}}{\pi} kt_R V_{aR} \cos(a_R) - R_R I_{dc} \quad (2.26)$$

$$P_R = V_R I_{dc} \quad (2.27)$$

$$\varphi_R = \cos^{-1} \left(\frac{\pi V_R}{3\sqrt{6} kt_R V_{aR}} \right) \quad (2.28)$$

$$Q_R = P_R \tan(\varphi_R) \quad (2.29)$$

and for the inverter:

$$V_I = -\frac{3\sqrt{6}}{\pi} kt_I V_{aI} \cos(a_I) + R_I I_{dc} \quad (2.30)$$

$$P_I = V_I I_{dc} \quad (2.31)$$

$$\varphi_I = \cos^{-1} \left(\frac{\pi V_I}{3\sqrt{6} kt_I V_{aI}} \right) \quad (2.32)$$

$$Q_I = P_I \tan(\varphi_I) \quad (2.33)$$

The relations giving the reactive power are approximate, given that they do not include the reactive power associated with harmonics. Finally for the dc transmission line:

$$V_R - V_I = R_E I_{dc} \quad (2.34)$$

The quantity R_E includes the dc line resistance, with the addition of an equivalent resistance representing converter losses. It should be noted that the quantities R_R and R_I are not real resistances and thus should not be included when estimating interconnection losses.

As can be deduced from the above equations there are four control parameters in the system: the converter ignition angles and their transformers tap ratio. For any given power transfer requirement the solution depends on the control strategy. The most commonly used control mode uses the rectifier to achieve a desired dc current (power) value, and the inverter at a constant ignition angle [15,16]. Consequently the inverter operates at the maximum a_I value, while a_R is adjusted to achieve the desired active power. Then t_R is adjusted as much is needed to keep a_R within the allowable operation range, while t_I is adjusted to minimize reactive power consumption. Reversing these roles of inverter and rectifier is also possible. Whether or not this is done, typically depends on reactive power compensation and losses cost on the ac sides of the system [16].

2.6.2 Self Commutated Voltage Source Converters

A simple schematic of a voltage source converter may be seen on Fig. 2.25. While equation (2.34) is still valid for this type of interconnections, active and reactive power, and consequently voltage output, on both sides of the converter depends simply on the control signals. No particular equations related to the converter are involved here, with the exception of constraints limiting the ac voltage amplitude. In order to control the active power transfer the dc voltage of the receiving terminal is

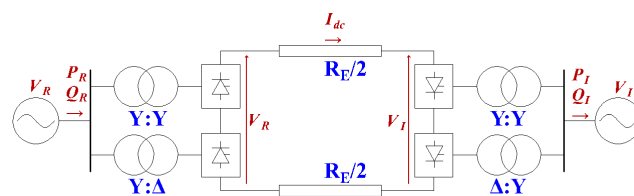


Fig. 2.24. Thyristor 12-pulse current source converter monopolar dc-link.

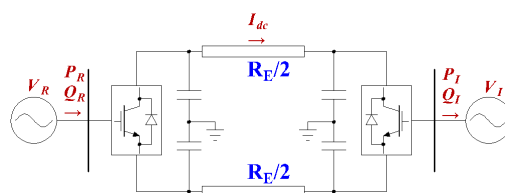


Fig. 2.25. An IGBT voltage source converter monopolar dc-link.

decreased to an appropriate level. A detailed description of control concepts utilized in VSC based dc-links, especially in the case of weak ac systems interconnections, may be found in [19,20].

2.7 DC Link Design Aspects

In the previous sections the basic equations governing the steady state behavior of a dc-link have been presented. In addition to that however it is of interest to see how the models' parameters, and particularly investment costs and energy losses, are affected by interconnection design considerations, and more specifically how they vary as a function of the dc-link size. Thus, in the following paragraphs, some of the most important design aspects are briefly discussed and related equations are presented as necessary.

2.7.1 Converter Components

Typically a multitude of filters are required for the correct operation of each converter. The type and size of harmonic filters on each side of a converter depends of course on the converter type. Additional reactors may be employed on the ac and dc side in order to limit currents rise due to faults or provide reactive compensation for capacitive filters during low load operation. Surge arresters placed between phases or on each valve offer protection in case of overvoltage. Each converter valve consists of multiple electronic switches connected in series. The number of switches depends on the dc-link voltage which in turn is determined based on the expected power transfer through the dc-link. This is also the case for the transformer size. As can be expected costs increase as the interconnection nominal power increases. A good introduction on transformer characteristics selection, valves cooling and signaling, insulation coordination, and dc-link telecommunications required for the converter controls may be found in [1].

2.7.2 Underground / Submarine Cables

More often than not submarine cables used in interconnections are made specifically to meet the needs of a specific project. Only in rare cases are they purchased in standardized cross-sections [21]. In any case the dc cable is composed of the following basic parts :

Conductor: Typically consists of copper or aluminum. For its construction several options exist. It may be a solid conductor (for cross-sections up to about 400 mm^2), or most commonly made from stranded round wires. When a large cross-section is required however it is more economic to construct the conductor from multiple smaller conductors, which combine to form a single circular one (so called profiled conductor). Hollow conductors for oil-filled cables are also a possibility. These have improved heat dissipation and for a specific voltage level require a lower insulation thickness. Depending on the conductor type, the electric conductivity (and thus resistance) of conductors made from the same material can be expected to differ.

Insulation: The most common option is mass paper insulation. It is the oldest and most commonly used insulation for submarine cable systems and can reach as high as 600 kV , for theoretically unlimited distances. One issue with mass impregnated paper insulated cables however is that cavities can form in the dielectric, resulting in premature aging of the cable. A solution is provided by gas or oil filled paper insulated cables. However due to the fact that a specific fluid pressure has to be maintained, correct operation cannot be guaranteed for distances over $40\text{-}60 \text{ km}$. Finally extruded XLPE insulation has been gaining popularity in recent years and can reach as high as 550 kV . However their use is limited by the fact that flexible joints for very high voltage levels are not available. An outer metallic sheath protects insulation from water.

Armoring: This is constructed from metal wires wound around the cable. It should be able to withstand tensile forces during cable laying (which are typically much larger than the static forces on the cable), and in addition provide sufficient mechanical protection from external factors (e.g. ship anchors). The armor wires are coated with zinc and bitumen to prevent corrosion from sea-water. In turn, these layers are protected by an additional outer polymeric serving or a serving made from wound yarn layers.

The overall cable ampacity depends on the thermal properties of its individual components. Considering a single cable layer, for example the insulation, then the temperature drop $\Delta\Theta$ across that layer is equal to:

$$\Delta\Theta = T \cdot W \quad (2.35)$$

where W is the thermal energy generated in the cable. In dc cables in steady state conditions this is equal to the Joule losses. Assuming a cylindrical cable structure then the thermal resistance per unit length is equal to:

$$T = \frac{\rho_{th}}{2\pi} \ln \frac{r_o}{r_i} \quad (2.36)$$

where ρ_{th} the material's thermal resistivity, r_o the outer and r_i the inner layer radius. In addition to the thermal resistance each cable layer may be associated with a certain thermal capacitance. Subsequently the thermal model of the cable can be essentially represented by an electrical equivalent [22], with the thermal resistances of the different layers connected in series and thermal capacitances connected in parallel. Thus, for example, for a typical submarine dc cable the following relation applies:

$$\Delta\Theta = I_n^2 R \sum_{i=1}^4 T_i = \frac{T_n^2}{V_n^2} R \sum_{i=1}^4 T_i \quad (2.37)$$

where T_n the nominal dc-link power, V_n the nominal dc-link voltage, T_1 the insulation thermal resistance, T_2 the thermal resistance of the layers between the insulation metallic sheath and the cable armoring, T_3 the thermal resistance of the cable outer serving, and T_4 the thermal resistance between the cable and sea floor. The thermal resistances T_1 to T_3 are estimated based on equation (2.36), while T_4 varies depending on the cable burial depth and proximity of other cables [22]. As is well known the electrical resistance R is inversely proportional to the conductor cross-section. Finally $\Delta\Theta$ is the difference between the maximum permissible conductor temperature and the ambient temperature.

Insulation material and thickness is selected so that a certain design stress is achieved. It should be noted that in dc currents, the dielectric strength is significantly affected by temperature, and thus varies depending on the cable operating conditions. In addition increasing insulation thickness over the minimum required can increase the cable life time. Details on the design process and various insulation breakdown mechanisms may be found in [21,23]. The type of the material used in the armoring as well as the resulting diameter of the cable depend on the mechanical properties which are required, so that the cable can withstand all forces that can be expected during operation and especially laying.

Determining the cable parameters, i.e. the conductor cross-section, and thickness and type of each subsequent layer, is essentially a problem of optimization. The objective would be to minimize installation costs, and if an adequately good estimate for the projected cable usage exists, then this might also be taken into account [24]. As the above discussion indicates for such calculations a large number of parameters are required and in addition the relevant cost functions. Complete data at the time of writing of this work were not available. Consequently in order to estimate the interconnection losses typical data taken from [25] are used. These are approximated with a curve $k = c_1/T_n + c_2$ as illustrated on Fig. 2.26. It should be noted that converter losses are also included in this relation.

2.7.3 Overhead Lines and Earth Electrodes

Typically HVDC overhead lines are bipolar. Design of line towers and line insulation involves considerations on the required rights-of-way, losses and reliability. Details may be found in [1]. An

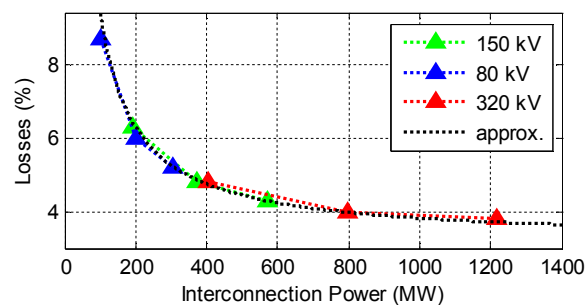


Fig. 2.26. Total losses for a 100 km interconnection transmitting its nominal power as a function of its nominal power.

additional factor contributing to losses, which is not present in underground or submarine cables, is the corona phenomenon. The magnitude of the resulting losses depends on various parameters (voltage levels, weather characteristics etc.). However these losses can be considered small compared to Joule losses and therefore do not need to be accounted for separately.

Connecting nodes of the dc system to the earth is necessary to help the system establish a reference voltage point, required for insulation coordination and overvoltage protection design. This is accomplished by suitable earth electrodes. In a monopolar link the electrodes carry the nominal dc current. In a bipolar dc interconnection, despite current balancing control of the two poles, there is always a current flowing from the neutral point to the ground. In addition to the expected current flows, selection of a suitable electrode type is based on consideration of the ground thermal characteristics, resistance and expected corrosion. Any effect on the normal operation of the interconnection (e.g. on losses) that the electrode design has may be assumed to be of limited importance.

2.8 Interaction Between AC and DC Systems

A large variety of interactions may exist between ac and dc systems. Their analysis can be quite complex. These interactions and their importance are typically dependent on the ac system strength. A system may be considered weak if it has a high impedance, or low mechanical inertia. A basic assessment of the system strength and related interactions is possible through suitable indices. One most commonly used such index is the short circuit ratio (*SCR*), defined as follows:

$$SCR = SCL/T_{dc} \quad (2.38)$$

$$SCL = E_{ac}^2/Z_{ac} \quad (2.39)$$

where E_{ac} is the commutation bus voltage, Z_{ac} the system's Thevenin equivalent impedance, and T_{dc} the power transferred through the dc-link. It is of note that as operating conditions vary so will *SCR*. Thus its estimation only on a few specific cases may not give a sufficiently good description of the ac system. Additionally this index is often replaced by the effective short circuit ratio *ESCR*, which also takes into account the dc-link's capacitor and filter banks [1]. As the *ESCR* decreases multiple issues arise, especially if the standard line commutated converters are used:

Dynamic Overvoltages: In case of dc current interruption the reactive power consumed drops to zero, while reactive power generated by compensating capacitors is still produced. This in turn might result in significant overvoltage and thus a higher insulation level is required, imposing an economic penalty. Furthermore the overvoltage might result in damages to nearby customer equipment.

Flicker: Due to the high ac system impedance voltage will be very sensitive to load changes. The same is true during switching of shunt capacitors which may cause significant voltage variations in the vicinity of the compensation equipment.

Voltage Stability: Again due to the high impedance, voltage control and recovery from faults can be very difficult. Especially if available compensation comes solely in the form of capacitor banks.

Resonance: In an electrical network with capacitances and inductances (which is the case for the harmonic filters and reactive power compensation components of the dc-link) frequency resonance phenomena may be observed. Typically high frequencies are adequately damped. If however the resonant frequency is low, then related low order harmonics may be amplified to unacceptable levels. The resonance frequency is dependent on the system *SCR*:

$$\omega_r = \omega_0 \sqrt{\frac{SCL}{Q_c}} = \omega_0 \sqrt{\frac{SCR}{k}} \quad (2.40)$$

where k is the ratio of reactive to active power output of the dc-link. Typically during normal operation is on the order of 0.6. In systems with low *SCR* low resonant frequencies, insufficiently damped, may be observed.

When supplying isolated systems through a dc-link local conventional generators are displaced. This effectively reduces system inertia. Thus frequency related issues may become more acute. An additional index related to this issue is the effective inertia constant defined as:

$$H_e = \frac{J_i}{T_{dc}} \quad (2.41)$$

where J_i is the total power system inertia in *MW s*, which also varies during system operation. It should be noted that this index along with *SCR*, gives a rough picture of the system's behavior which can be indicative of general trends in the system's response during various phenomena. In systems with low

values of these indexes it should be clear that a voltage source converter based solution should be preferable for a potential interconnection. In addition frequency support control schemes from the interconnection might be in order. For a realistic assessment of the system's behavior detailed simulations are required. Finally control related issues may also arise between a dc-link and conventional generators or FACTS, or between different dc-links, resulting in various types of oscillatory behavior or voltage instability.

Power System Probabilistic Assessment

3.1 Introduction

Traditionally most power system studies are based on specific (worst case) scenarios analysis. However this does not give a complete picture of the overall system behavior. Thus taking probabilities into account is essential. Traditional analytical probabilistic approaches, though fast, are hardly adaptable to complex systems, and often presuppose simplifications that may significantly affect the results. An alternative is provided by Monte Carlo methods, which involve simulating a significant number of system states. This however, thanks to modern computers increased computational capabilities, is possible within an acceptable time frame. Of course certain simplifications might still be required. A Monte Carlo simulation involves a three step loop:

1. Generate a sample system state.
2. Solve the current state.
3. Update indices and check convergence. Go to step 1 if convergence has not been reached.

In the following sections the basics of the method will be presented, and its properties will be discussed from a transmission expansion evaluation point of view. This chapter focuses on the first and last of the above steps. The second step and the indices used will be analyzed in subsequent chapters.

3.2 Monte Carlo Simulation Approaches

Essentially, what a Monte Carlo process does, is generate a set of possible system states. This is done through a suitable sampling process [26]. Depending on whether or not a generated system state sample is related to the previously generated state samples, the method can be either sequential or non-sequential.

Sequential Monte Carlo: In sequential MC each state sample is assumed to have a certain duration. Typically this is assumed equal to 1 hour, assuming that system changes within this time period are very small. By sampling suitable probability distributions describing the behavior of each system component, system changes from one simulation hour to the next can be calculated. Thus the detailed system history is known for the total duration of the simulation. This approach enables the easy incorporation of any system component peculiarities at any level of detail. Unit commitment schemes may also be taken into account giving a more detailed simulation of the system. However a significant amount of data is required. Furthermore the additional routines (such as unit commitment) and the fact that convergence is slow compared to a non-sequential approach (due to the chronological continuity of the generated states), the computational burden is significantly higher.

Non-sequential Monte Carlo: In its simplest form the non-sequential approach involves sampling the probability distributions related to the various system components to determine their status, and consequently the system state. Each state sample generated in this way is completely independent of previous samples. This method requires much less data than the sequential approach and in general converges faster. Of course any system operation that depends on the system state over multiple hours may not be taken into account.

In the problem of transmission expansion, in order to assess the benefits of any possible scenario, the effects on the system operation have to be evaluated for a particularly long time duration. Thus computational speed is an important factor. In addition, it is difficult to predict much of the required data

for future time periods. A sequential approach would require a significant amount of time to converge and much guesswork as far as data is concerned. For these reasons in this work a non-sequential Monte Carlo is preferred. The only disadvantage of any importance is the fact that it is not possible to incorporate any kind of unit commitment considerations into the method. Due to the turn on/off costs of conventional generators and their typical minimum up/down times, a different conventional generation configuration might be covering the load at any specific moment, that what might be estimated by a single instance optimal load flow. This in turn can affect system operational costs, which is the main factor of interest and will be discussed further in the following chapter.

3.3 State Samples Generation

Each state sample consists of status information of all power system components. It should be noted that an algorithm to generate pseudo-random numbers following a uniform distribution is required. While such an algorithm won't be presented in this text, details may be found in [26,27]. Starting from the uniformly distributed random numbers it is desirable to generate random numbers following other distribution functions. In addition it is required to generate random numbers with a certain correlation. Methods to do these will be discussed in the following sections along with the specifics concerning each power system component.

3.3.1 Inverse Transform Method

The inverse transform method is a simple way to generate random numbers from any probability distribution given its cumulative distribution function F . It is assumed that F^{-1} may be defined. The method follows two simple steps:

1. Draw a number $U_i \sim U(0,1)$.
2. Calculate $X = F^{-1}(U_i)$.

Given that U is uniformly distributed then X follows the distribution F .

3.3.2 Correlated Random Numbers Generation

Generating independent (non-correlated) sets of random numbers is a straightforward process. The only requirement is to generate independent uniformly distributed sets of numbers and then use the inverse transform method. However, when a certain degree of dependence (correlation) is desired, a more complicated approach is required. One possible solution in this problem may be derived using copula theory [27]. Before tackling the general problem, a brief review of two commonly used correlation measures follows. The first is the well known Pearson correlation. Let X and Y be two random variables, then the Pearson correlation coefficient is given by the relation:

$$\rho_P = \frac{\text{cov}(X,Y)}{\sigma_X \sigma_Y} \quad (3.1)$$

This is a measure of the linear relationship between the two random variables. An alternative way to measure variable dependence are the rank correlation coefficients. One such example is the Spearman correlation coefficient ρ_S which may be calculated by converting the random variables to ranks and then applying the relation of Pearson coefficient [28]. The Spearman correlation coefficient is a measure of the monotonic relationship between the random variables. An important property of rank correlation coefficients is that if the inverse transform method is applied to the random numbers, these coefficients remain unchanged. The reason is that this transformation is made through the cumulative distribution function, which is monotonic. On the contrary, Pearson correlation cannot be guaranteed to remain unchanged through this transformation.

Now let us assume that the target is to generate n sets of m random uniformly distributed numbers with covariance matrix Σ . The following procedure is required:

1. Calculate the Cholesky decomposition $\Sigma = \mathbf{A} \cdot \mathbf{A}^T$.
2. Generate independent and identically distributed $U_1, \dots, U_n \sim N(0,1)$.
3. Calculate $\mathbf{X} = \boldsymbol{\mu} + \mathbf{A}\mathbf{U}$.

Then $\mathbf{X} \sim \mathbf{N}(\boldsymbol{\mu}, \Sigma)$. The final two steps have to be repeated m times. Given that the Pearson correlation matrix is nothing more than a normalized covariance matrix, generating normal random numbers with a

standard Pearson correlation is simple. If a specific Spearman rank correlation is desired then this may also be easily achieved by taking into account that for the normal distribution [29]:

$$\rho_S = 2 \sin\left(\frac{\pi}{6} \rho_P\right) \tag{3.2}$$

This relation also provides the basis for generating correlated uniform random numbers. It should be noted that for the uniform distribution $\rho_S = \rho_P$. Thus the following steps have to be followed:

1. Calculate the adjusted covariance matrix Σ^m based on (3.2).
2. Generate random numbers $\mathbf{U} \sim \mathbf{N}(\mathbf{0}, \Sigma^m)$.
3. Calculate $\mathbf{X} = F_n(\mathbf{U})$, where F_n is the normal cumulative distribution function.

The generated random numbers will have the desired distribution and correlation. In order to generate correlated random numbers of an arbitrary distribution, the correlated uniform random numbers may be used with an additional application of the inverse transform method. As mentioned before only rank correlation will be preserved. Therefore if a certain Pearson correlation is required, a relation should be established between Spearman and Pearson correlation for the arbitrary distribution.

3.3.3 Power System Components Modeling

Considering a system with k demand buses, n conventional generators, m wind parks, q ac transmission lines and p dc interconnections, each sample system state is a vector of the following form:

$$\mathbf{S} = \left[\begin{array}{c|c|c|c|c} \text{demand} & \text{conv. gen.} & \text{wind gen.} & \text{transmission} & \text{dc-links} \\ \hline P_1^d & \dots & P_k^d & S_1^g & \dots & S_n^g & S_1^w & \dots & S_m^w & S_q^t & \dots & S_q^t & S_p^t & \dots & S_p^t \end{array} \right] \tag{3.3}$$

For each state the demand level in each bus, the maximum available power of the various generating units, and the maximum transfer capability of transmission components has to be estimated. The estimation procedure is different for the various system components as described in the following.

Power System Demand: First let us assume a single bus case. Required data is the load duration curve for the specific bus, such as the one illustrated in Fig. 3.1. Since the duration curve is essentially the inverse cumulative distribution function of the demand, the inverse transform method is used to generate demand samples. In a power system with multiple buses, on the assumption that demand of different buses is fully correlated, a single duration curve may be used to estimate the total demand. This is then distributed among different buses. Alternatively if correlation between different buses is known their behavior may be approximated by using different duration curves and the method described in the previous section.

Conventional Generation: Each unit is assumed to reside in one of two states: available for commitment or unavailable. The forced outage rate (*FOR* or probability of unavailability) is required for each generator. The unit status or available power is determined by drawing a number $U_i \sim U(0,1)$ and using the following function:

$$S_i^g = \begin{cases} P_i^{max} & \text{if } U_i \geq FOR \\ 0 & \text{if } U_i \leq FOR \end{cases} \tag{3.4}$$

This model may be easily extended to include additional unit states (e.g. derated states) if required.

Wind Generation: As discussed in [30] there are several important aspects as far as wind generation modeling for reliability and probabilistic power system studies in general is concerned. First and

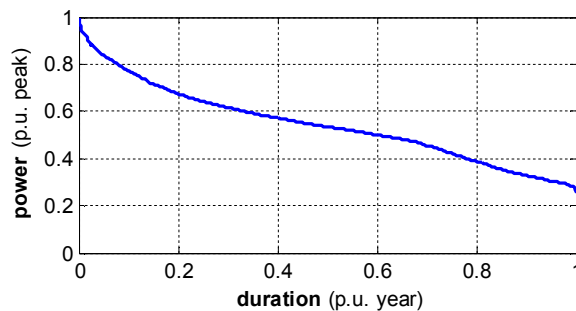


Fig. 3.1. Power demand duration curve.

foremost wind speed simulation is an important aspect. The non-sequential approach simplifies things as wind speed autocorrelation does not need to be modeled. Thus sampling the wind speed distribution of each wind park will suffice. Of course correlation between different wind parks is still an important factor. Assuming that the wind speed v_i^w of a wind park is known then the available power has to be estimated taking into account the wake effects resulting from the wind turbines spatial arrangement within the park area. The simplest approximation for a single wind turbine power characteristic may be given by the following relation:

$$P^{w/t} = \begin{cases} 0 & v_i^w \leq v_i^{cut-in} \\ c_2 (v_i^w)^2 + c_1 v_i^w + c_0 & v_i^{cut-in} \leq v_i^w < v_i^{nom} \\ P_i^{nom} & v_i^{nom} \leq v_i^w \leq v_i^{cut-out} \\ 0 & v_i^{cut-out} \leq v_i^w \end{cases} \quad (3.5)$$

The constants c_2, c_1, c_0 may be found in [31]. The total wind park output can then be estimated by:

$$P_i^w = n_{wk} n_{wn} P^{w/t} \quad (3.6)$$

where n_{wk} is an efficiency coefficient related to wake effects on the order of 90-95% [30], and n_{wn} is the number of wind turbines. If a more detailed power versus wind speed characteristic (derived from measurements [32]) exists for a wind park it may be used instead. Examples of wind speed cumulative distribution and wind turbine characteristics may be seen on Fig. 3.2 and Fig. 3.3.

As can be expected the wind park state depends also on wind park availability. This may be divided in two components: wind turbine availability, and availability of the wind park itself. The former depends on the characteristics of each generator and also on the wind park's internal network configuration. The latter depends on the way the wind park is connected to the high voltage network. In this work only this second aspect will be considered by using a forced outage rate for each wind park. In a similar fashion to conventional generators wind park availability is determined by drawing $U_i \sim U(0,1)$ and using the function:

$$S_i^w = \begin{cases} P_i^w & \text{if } U_i \geq FOR \\ 0 & \text{if } U_i \leq FOR \end{cases} \quad (3.7)$$

The effects of individual wind turbines outages may be easily incorporated into the method, as long as data is available, using a simplified multi-state model similar to the one described in [33].

AC Transmission System: The typical transmission line may be represented by a two state model, similar to that of the conventional generators. According to [34] for a 150 kV line an average of 0.3-0.5 faults per 100 km may be expected on an annual basis. The average restoration time may be around 12-13 hours. This yields a very low forced outage rate. While major transmission line outages may have significant impact on reliability indices it may be assumed that their impact on the average marginal system costs is limited.

DC Interconnections: Reliability constitutes an important part of interconnection design [35]. For example type of cable armoring, thickness of insulation, interconnection configuration, provision of spare parts are a few of the parameters that will affect the expected number and duration of outages. Apart from such design considerations however, especially for submarine interconnections, other factors (e.g. environmental conditions, sea traffic [21,36]) may have an impact on availability. In this work the interconnection is assumed to be always available, on the grounds that the typical outage can

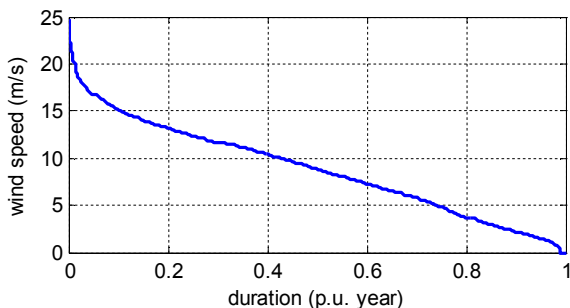


Fig. 3.2. Sample wind speed duration curve.

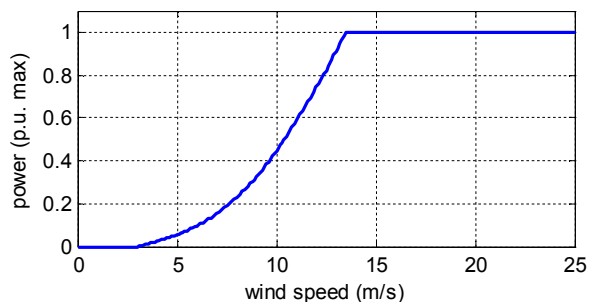


Fig. 3.3. Sample wind turbine power output characteristic.

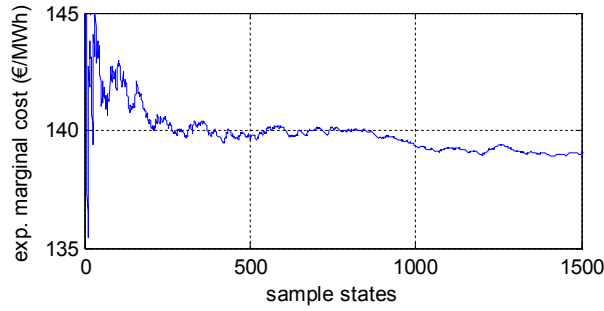


Fig. 3.4. Indicative results for the estimation of the expected marginal system cost of a test power system.

be quickly repaired, without having a significant effect on the average system cost. An exception would be an outage due to cable failure. In submarine interconnections this might result in weeks or months on outage as both specialized equipment and favorable weather are required. As long as data are available dc-link failures may be easily taken into account, but since under certain conditions the interconnection unavailability may be prolonged and drastically change the system operation, it is this author's opinion that it should be better separately evaluated.

3.4 Convergence Conditions

Let X be a set of values corresponding to a certain system quantity, which are calculated through the solution of the generated state samples. Typically in a Monte Carlo simulation the quantity of interest is its expected value $E(X)$. While generation of a few additional samples does not guarantee a smaller error in the estimate of the expected value of X (as illustrated in Fig. 3.4), the confidence interval is bound to decrease. The point of setting a convergence criterion is to strike a balance between accuracy and computational cost (or number of generated samples). One such criterion is the coefficient of variation of the index $E(X)$, defined as follows [26]:

$$\alpha = \frac{\sigma(X)}{\sqrt{n}} \frac{1}{E(X)} \quad (3.8)$$

where n the number of samples and σ the standard deviation. The first fraction is the standard error of the mean value of X , which may be interpreted as an estimate of the standard deviation of the error in the sample mean relative to the true mean. After the solution of each generated state sample the coefficient α is calculated, and if found smaller than an arbitrarily set value (typically at most around 5%) the simulation terminates. Both the expected value and the standard deviation may be calculated recursively by using the following relations:

$$E(X_n) = \frac{E(X_{n-1})(n-1) + x_n}{n} = E(X_{n-1}) + \frac{x_n - E(X_{n-1})}{n} \quad (3.9)$$

$$\sigma(X_n) = \sqrt{E(X_n - E(X_n))^2} = \sqrt{E(X_n^2) - E(X_n)^2} \quad (3.10)$$

In this way the coefficient of variation may be updated as the new sample x_n comes up, without requiring to store all previous values.

Power System Steady State Analysis

4.1 Introduction

As described in the previous chapter, for each system state sample, the demand in system buses, generating sources availability and output capability, transmission system components availability and transfer capability are known. Subsequently it is required to estimate how much demand is finally covered and by which generating sources. This involves solving the steady state equations describing the system. Furthermore the solution should be optimal from a cost point of view, while satisfying certain security constraints. In the following sections this optimal power flow formulation and solution method will be analyzed, as always from a transmission expansion perspective. System marginal costs are assumed to be the key factors that determine overall operational costs. Thus at the end of any calculations these are the quantities that need to be known.

4.2 Power Flow Equations

Let us consider a system of n buses. Let \mathbf{I} be a $n \times 1$ vector with elements the current injection phasors of each bus, and \mathbf{V} a $n \times 1$ vector of the bus voltage phasors. Then the following relation stands [15]:

$$\mathbf{I}_b = \mathbf{Y}\mathbf{V}_b \quad (4.1)$$

The matrix \mathbf{Y} is the node admittance matrix, with Y_{ij} the negative sum of all admittances between nodes i and j , and Y_{ii} the sum of admittances terminating at bus i . Constant impedance loads may be included in the node admittance matrix. For the complex power injections:

$$\mathbf{S}_b = \text{diag}(\mathbf{V}_b)\mathbf{I}_b^* = \text{diag}(\mathbf{V}_b)\mathbf{Y}^*\mathbf{V}_b^* \quad (4.2)$$

The set of non-linear equations described by (4.2) constitutes the full ac load flow equations. However there are simpler alternatives. The simplest approach is the so called dc load flow which comes with the following assumptions:

- Bus voltages are assumed to be equal to 1 p.u. and the equations related to reactive power are neglected.
- Branch resistances are much smaller than branch reactances and shunt reactances to the ground may be neglected.
- Voltage angle difference between two buses of a line is small, thus $\sin\delta_{ij} \approx \delta_i - \delta_j$ and $\cos\delta_{ij} \approx 1$.

Let us consider the simplest model of a transmission line k , between nodes i and j , as described by the following equation:

$$\mathbf{V}_i - \mathbf{V}_j = \mathbf{I}\mathbf{Z}_k \quad (4.3)$$

The apparent power from node i to j is then:

$$\begin{aligned} S_i &= \mathbf{V}_i \frac{(\mathbf{V}_i - \mathbf{V}_j)^*}{\mathbf{Z}_k^*} = V_i e^{j\delta_{ij}} \frac{(V_i e^{-j\delta_{ij}} - V_j)}{Z_k e^{-j\theta_k}} = \\ &= \frac{1}{Z_k} (V_i^2 e^{j\theta_k} - V_i V_j e^{j(\theta_k + \delta_{ij})}) \end{aligned} \quad (4.4)$$

Consequently the real power is given by:

$$T_i = \frac{1}{Z_k} (V_i^2 \cos(\theta_k) - V_i V_j \cos(\theta_k + \delta_{ij})) \approx \frac{\delta_i - \delta_j}{X_k} \quad (4.5)$$

As a result the transmission system equations may be written as:

$$\mathbf{P}_b = \mathbf{B}\boldsymbol{\delta} \quad (4.6)$$

Where \mathbf{P}_b is a $n \times 1$ vector with the active power injection in each bus, $\boldsymbol{\delta}$ the $n \times 1$ bus angles vector, and \mathbf{B} a simplified bus admittance matrix. with $B_{ij} = -1/X_{ij}$ and $B_{ii} = -\sum_{j=1 \dots n} B_{ij}$. The dc load flow cannot be used in cases where voltage and reactive power play a defining role. However it gives an adequately good representation of active power flows in the system, while offering a significant reduction in computational cost, as the problem is now linear and has only half as many equations as the full ac load flow. Given the large number of state samples that are required to be solved in order to determine the optimal investment, this approach will be used in this work.

4.3 Optimal Power Flow Formulation

The equations described in the previous section have multiple solutions. One solution that would possibly be applied is one that minimizes system operation costs and load curtailments. This may be expressed by the following cost function:

$$f = \mathbf{c}_c \mathbf{P}_c + \mathbf{c}_w \mathbf{P}_w - \mathbf{c}_d \mathbf{P}_d \quad (4.7)$$

where \mathbf{c}_c and \mathbf{c}_w costs per *MWh* associated with conventional and wind generation respectively, while \mathbf{c}_d a penalty factor associated with load shedding. In addition the following are the basic constraints which have to be taken into account:

$$\mathbf{C}_c \mathbf{P}_c + \mathbf{C}_w \mathbf{P}_w - \mathbf{C}_d \mathbf{P}_d = \mathbf{B}\boldsymbol{\delta} \quad (4.8)$$

$$\mathbf{P}_c^{min} \leq \mathbf{P}_c \leq \mathbf{P}_c^{max} \quad (4.9)$$

$$\mathbf{0} \leq \mathbf{P}_w \leq \mathbf{P}_w^{max} \quad (4.10)$$

$$\mathbf{0} \leq \mathbf{P}_d \leq \mathbf{P}_d^{max} \quad (4.11)$$

$$|\mathbf{B}_t \boldsymbol{\delta}| \leq \mathbf{T}^{max} \quad (4.12)$$

Equation (4.8) describes the active power balance in the system. The matrix \mathbf{C}_c is a conventional generators connection matrix where $C_{c,ij} = 1$ if the generator j is connected to bus i , and $C_{c,ij} = 0$ otherwise. The matrices \mathbf{C}_w and \mathbf{C}_d are similarly defined. The shadow prices associated with these equations give the marginal generation cost in each bus. Equations (4.9) to (4.11) describe typical technical constraints related to generation and demand. Finally (4.12) deals with transmission lines power transfer limits. For the matrix \mathbf{B}_t if line k connects buses i and j then $\mathbf{B}_{t,ki} = -\mathbf{B}_{t,kj} = 1/X_{ij}$.

The above optimal power flow formulation may be found lacking in three respects. First, losses have not been taken into account. Second, dc interconnections included in the system are not yet modeled. Third, security constraints are not included. These might significantly affect system costs and planning, especially when dealing with smaller systems. All these factors will be addressed in the following. Finally it should be noted that a Monte Carlo state sample indicates conventional generators availability. Equation (4.9) implies that, due to technical minimums, which generators are operational out of those available has to be known in order to reach a solution. This means that an integer optimization problem would have to be solved. In order to avoid this, it is possible to set the technical minimums to zero [37]. As a result marginal system costs will tend to be overestimated.

4.3.1 AC Transmission Losses Approximation

Given that line resistances are neglected from matrix \mathbf{B} , transmission system losses are not included in (4.8). An approximation however is possible in the following way. In a similar fashion to equation (4.5) the real power at node j may be expressed as:

$$T_j = \frac{1}{Z_k} (V_i V_j \cos(\theta_k - \delta_{ij}) - V_j^2 \cos(\theta_k)) \quad (4.13)$$

The losses over this line are then [38]:

$$\begin{aligned} P_{l,ij} &= T_i - T_j = \frac{\cos(\theta_k)}{Z_k} [(V_i^2 + V_j^2) - 2V_i V_j \cos(\delta_{ij})] \approx \\ &\approx \frac{2R_k}{Z_k^2} (1 - \cos(\delta_{ij})) \approx \frac{4R_k}{X_k^2} \sin^2\left(\frac{\delta_{ij}}{2}\right) \approx R_k T_i^2 \end{aligned} \quad (4.14)$$

Variants of the above equation are used in several papers for losses estimation in power system planning [37,39,40,41]. The losses of each line are equally allocated to its two connecting buses as suggested in [6]. Consequently equation (4.8) may be rewritten as:

$$\mathbf{C}_c \mathbf{P}_c + \mathbf{C}_w \mathbf{P}_w - \mathbf{C}_d \mathbf{P}_d - \mathbf{C}_l \mathbf{P}_l = \mathbf{B} \delta \quad (4.15)$$

where \mathbf{P}_l is the line losses vector. For the matrix \mathbf{C}_l , if line k connects buses i and j then $\mathbf{C}_{l,ik} = \mathbf{C}_{l,jk} = 1/2$. Various methods for linearization of the above equations, if so desired, are presented in the aforementioned papers.

4.3.2 DC Interconnection Modeling

As has been analyzed in previous chapters the equations describing the dc-link vary depending on the converter type and even depending on the switching method. Including the full dc-link equations as described in the previous chapters is a straightforward procedure [42,43,44]. It should be noted however that from a power flow perspective there are ultimately three characteristics of interest that are expected to affect system costs:

Losses: These represent the cost of transferring power over the interconnection and as such, they are a cost defining factor. Especially if the distance spanned by the interconnection is long. Based on equation (2.34) if T_{dc1}^{i-} and T_{dc2}^{i+} the power absorbed and injected respectively at the two connected buses of the dc-link i , then:

$$T_{dc1}^{i-} - T_{dc2}^{i+} = R_E I_{dc}^2 \quad (4.16)$$

assuming that the interconnection is operated near the nominal dc voltage then:

$$T_{dc1}^{i-} - T_{dc2}^{i+} = \frac{R_{E,i}}{(V_{dc,i}^n)^2} (T_{dc1}^{i-})^2 = k_{dc}^i (T_{dc1}^{i-})^2 = P_{ldc1}^i \quad (4.17)$$

This equation is not valid for a reverse power flow. Thus the following equation has to be added:

$$T_{dc2}^{i-} - T_{dc1}^{i+} = k_{dc}^i (T_{dc2}^{i-})^2 = P_{ldc2}^i \quad (4.18)$$

along with the following constraints:

$$0 \leq T_{dc1}^{i-} \leq T_{dc}^{i,max} \quad (4.19)$$

$$0 \leq T_{dc2}^{i-} \leq T_{dc}^{i,max} \quad (4.20)$$

It follows that at an optimal solution $T_{dc1}^{i-} \cdot T_{dc2}^{i-} = 0$. As can be expected equation (4.15) has to be further modified as follows:

$$\mathbf{C}_c \mathbf{P}_c + \mathbf{C}_w \mathbf{P}_w - \mathbf{C}_d \mathbf{P}_d - \mathbf{C}_l \mathbf{P}_l - [\mathbf{C}_{dc1} \mathbf{T}_{dc1}^- + \mathbf{C}_{dc2} \mathbf{T}_{dc2}^- - \mathbf{C}_{ldc1} \mathbf{P}_{ldc1} - \mathbf{C}_{ldc2} \mathbf{P}_{ldc2}] = \mathbf{B} \delta \quad (4.21)$$

For the p dc-link, which connects buses i and j , then $\mathbf{C}_{dc1}^{ip} = -\mathbf{C}_{dc1}^{jp} = 1$ and $\mathbf{C}_{ldc1}^{jp} = 1$. The elements of matrices \mathbf{C}_{dc2} and \mathbf{C}_{ldc2} are similarly defined.

Power Transfer Limits: A large number of inequality constraints is involved with the full representation of a dc interconnection, related among others to dc current, dc voltage, firing angle limits, ac voltage, ac currents etc. These however may be adequately covered by the inequality constraints of the previous paragraph.

Reactive Power Output: This is of interest mostly when the full ac load flow equations are used. Simplified dc-link equations or dc power flow equations may be used under the assumption that voltage control in the interconnected buses is possible. In the case of the classic thyristor based converters this implies the provision of adequate compensation, while in the case of voltage source converters sufficient current margin to effectively control reactive power.

In order to reduce computational costs, and since the results are not affected in any essential way, the above simplified model is used in the optimal power flow.

4.4 Security Constraints Consideration

The optimal power flow as described until now does not include contingency criteria, or in other words the ability of the system to cope with generation or transmission outages. The relevant constraints if incorporated into the above method might significantly affect system costs and/or limit the utilization degree of the new equipment. System security considerations might deal with either steady state or with

dynamic stability system performance. Determining the required system security level as described by the various constraints is by itself an important issue.

Steady state security requirements in the case of generating unit outages are typically covered by maintaining a sufficient amount of reserve in the system. In the simplest case the total reserve should be such that it can cover the outage of any single generating unit. In larger systems the reserve target may be simply a certain percentage of the total demand. The problem becomes more complicated if the reserve target is calculated based on probabilistic criteria. Furthermore the ability of the transmission system to carry the reserve where it is required might also be an issue. Security requirements related to transmission outages have to do with ensuring that load curtailments will not be needed, or at least are minimized, when transmission lines trip. This might require deviating from the otherwise optimal power flow solution, by covering the load using a different combination of units.

Stability related security requirements deal with minimizing the probability of the system losing synchronism on a component outage. A basic issue is to translate stability considerations (typically a matter involving differential equations) into steady state constraints. In [45] neural networks are used to generate a function that estimates the system stability margin based on the current system state. Optimization constraints are added to the optimization problem based on this function. In [46] the generators swing equations are converted to a set of algebraic equations using a trapezoidal rule. Then constraints are imposed on the generator angles. A similar approach is used in [47], where a single equivalent machine model is derived to describe the power system generator angle behavior. In systems with high renewable sources penetration this problem becomes more complicated.

As can be expected, even when considering only an N-1 criterion the number of resulting contingency cases which have to be evaluated can be large enough, increasing significantly the computations required to complete a single optimal power flow case [48]. Therefore a few simplifications are in order, summed up in the following assumptions:

- Each isolated system is assumed to be a single area. This implies that ac transmission lines in that area are of sufficiently small length (or impedance), so that conventional generators have a coherent response, and no essential voltage stability issues are observed.
- Security constraints related to the ac transmission system within each area have either minimal impact on system costs, or the system structure is such that these constraints may not be taken effectively into account.
- There is no limitation to the short term power the ac transmission system in each area can transfer (for example when providing reserve from one area to another third area).

Under these assumptions the remaining security constraints that have to be considered are related to operating reserve, interconnection outages and renewable sources penetration levels.

4.4.1 System Reserve Level

Spinning reserve is perhaps the most prominent security requirement for any isolated system, allowing frequency control during daily demand variations and also limiting load curtailments during contingencies. When any generating components in a power system trip, there are two possible results [49]:

- If the spinning reserve is more than the capacity on outage then the load is served without any significant interruptions. Any load shed due to under-frequency protection system operation can be quickly restored, typically in less than 2 *min*.
- If the spinning reserve is less than the tripped capacity, then part of the load cannot be served unless new units start up. If fast generating units are available then interruptions will last from 10 to 20 *min*, else the interruptions may last several hours.

The period covered by each Monte-Carlo sample is assumed to be equal to one hour. As an approximation it is assumed that any contingency will affect only that particular hour. Availability of fast units is not considered, and load that cannot be covered remains curtailed for the whole hour. An obvious question is how much reserve is required, and how should it be distributed between system units. After all, maintaining an amount of reserve has a direct impact on system costs, and in the particular case of isolated systems planning can play a significant role [50].

Standard practice in power systems involves setting system reserves equal to either the largest power output among the generating units, or a certain percentage of system demand. This approach however gives neither a uniform security level as system conditions change, nor an economically optimal reserve. In [51] a probabilistic approach (perhaps the first) to setting reserve levels was proposed. This

involves calculating the probability that in a possible contingency, power loss will be greater than the reserve. The target is maintain during all operation hours a specific load curtailment risk, as expressed by the aforementioned probability. One disadvantage of this approach is that it may be detrimental from an economic point of view, as the reserve needed to meet the specified security requirements can be excessively large. As suggested in [52] a cost / benefit approach to setting reserve, especially in systems with high penetration of renewable sources, will give a better solution. Of course this presupposes the estimation of reserve benefits to either system reliability or costs incurred due to load shedding.

In order to estimate the probability of losing a specified amount of generation, or the expected energy not supplied (EENS) under a given system configuration, one has to estimate a table giving possible generation outages and the respective probability levels [53]. The process is simple:

1. Initialize the outage probability table: $PT_o = 0, PT_p = 1$.
2. Find a new generating unit with generating power P_g , reserve provision P_r and a outage replacement rate ORR_c . The outage replacement rate is the probability that the generating unit will trip and not be replaced within the lead time of interest t_o . Assuming that the time to failure is exponentially distributed then $ORR = \lambda t_o$, where λ is the unit's failure rate.
3. Update the outage probability table using the following relations: $PT_o = [PT_o + P_r; PT_o - P_g]$, $PT_p = [PT_p \cdot (1 - ORR_c); PT_p \cdot ORR_c]$.
4. Go to step 2 until there are no more generators left.

For a system with n generators the total number of states is 2^n . The computational requirements for a large system can be significant. The computations may be reduced by combining similar states or units with similar characteristics, or ignoring states with very low probability. Still, in [54] a capacity outage probability table is used to optimize reserve levels in an auxiliary optimization problem which is then combined with the full unit commitment problem. This method was further extended in [55] to take probabilistic load into account. In [56] it was suggested that the load carrying capability of generating units may be approximated using exponential curves. This idea was used in [57] where eventually the probabilistic reserve is taken into account in the unit commitment optimization through an additional linear constraint. This approach avoids the computational costs of the outage probability table during the optimization process, however can be inaccurate in systems with a small number of generators, or in systems with a high largest unit / system demand ratio. This of course is exactly the case in the interconnection of isolated systems as seen on Fig. 4.1. In [58] the expected generation loss is used as an indicator of possible outage costs, using a scaling factor to convert it into costs. The procedure for estimating this scaling factor however is not clarified. In [59,60] multiple calculations of EENS are required for reserve optimization, however an effective method for its calculation is not pointed out. Finally, criteria based on the system's primary frequency response are suggested in [61,62].

Overall setting the spinning reserve levels may be based either on cost by selecting a value of lost load (VOLL), or on maintaining a specific risk level. Let us consider the simple example where the power in a system is mostly covered by a single unit (or interconnection) such that for a single hour $EENS \cong P_g^i ORR^i$. From an economic point of view reserve will be provided as long as the cost per MW of reserve is lower than $VOLL \cdot ORR^i$. Respectively if the probability of load shedding is selected as a risk criterion then reserve will be provided, equal to P_g^i , as long as the desired risk level is lower than ORR^i . Given that in general both $VOLL$ and a risk criterion can be only arbitrarily selected, in this work

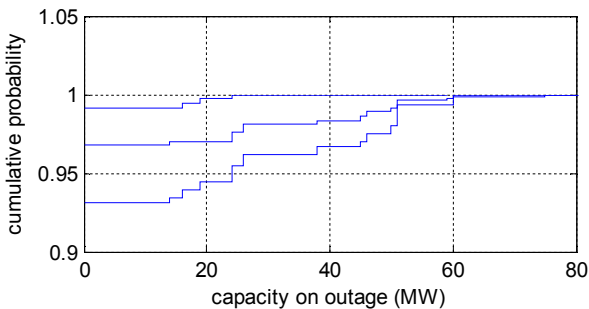


Fig. 4.1. Capacity on outage cumulative probability for various demand levels and unit configurations.

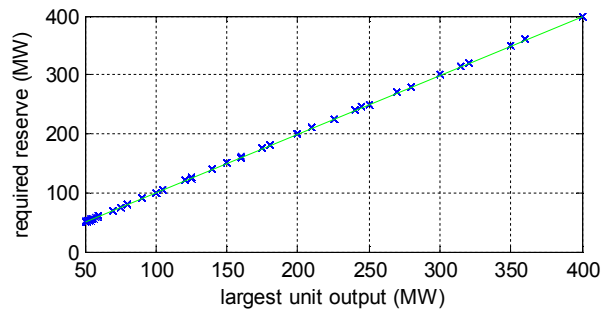


Fig. 4.2. Reserve requirements as a function of the largest generating unit in the system.

reserve levels are determined so that the probability of load shedding is lower than the lowest *ORR* of the committed units. This is equivalent to the standard N-1 criterion in case only a small number of units cover the demand, and essentially adjusts reserve to cover multiple generation outages in the case of systems with a large number of generators. This ensures an average number of load curtailments per year lower than $8760 \cdot ORR$. In order to illustrate this effect, the following simple process is considered:

- Pick a demand level at random
- For the given demand level determine at random renewable sources outputs.
- Solve the following simplified commitment problem with an addition of a zero cost generator with nominal power selected at random but no greater than the system demand:

$$\begin{aligned} \min \quad & \mathbf{c}_c \mathbf{P}_c + \mathbf{c}_w \mathbf{P}_w \\ \text{u.c.} \quad & \mathbf{I}_n \mathbf{P}_c + \mathbf{I}_m \mathbf{P}_w = \mathbf{I}_k \mathbf{P}_d \end{aligned} \quad (4.22)$$

- Estimate the capacity outage cumulative probability function.
- Find the reserve required to achieve the desired risk level.

The result for the test system is illustrated in Fig. 4.2. As can be seen the resulting reserve is roughly equal to the largest generating unit. This is to be expected as typically *ORR* has a small value, and due to the relatively small number of units covering the demand, multiple generating unit outages do not have a significant probability of appearance. Different systems might yield different such curves which may also vary as a function of the demand level. In the general case by calculating and approximating reserve requirements with suitable functions of the form $R_t = f(\max(P_c), \sum P_d)$, probabilistic reserve criteria may be incorporated in the system planning process. In systems where demand is covered by a small number of units, maintaining an $N - 1$ based criterion seems an adequately good reserve target for planning studies.

4.4.2 Reserve Cost and Distribution

While the above approach gives an estimate of the reserve required as a function of demand and the largest generating unit in the system, it does not indicate how that reserve should be distributed between operating units or between different areas / islands where transmission limitations are bound to exist. Obviously it should not be allowable for the same unit to provide a large amount of power and the system reserve. Given the fact however that generally the largest unit plays has the largest impact in reserve requirements a simple yet adequate approximation is given as follows. First the optimal power flow cost function is modified:

$$f = \mathbf{c}_c \mathbf{P}_c + \mathbf{c}_w \mathbf{P}_w + \mathbf{c}_R \mathbf{R} - \mathbf{c}_d \mathbf{P}_d \quad (4.23)$$

where \mathbf{R} a vector with reserve provided by various sources and \mathbf{c}_R the vector with the corresponding costs. Only reserve by conventional generators is considered. Similarly modified are the generation limits of conventional generators:

$$\mathbf{0} \leq \mathbf{P}_c + \mathbf{R} \leq \mathbf{P}_c^{max}, \mathbf{0} \leq \mathbf{P}_c, \mathbf{0} \leq \mathbf{R} \quad (4.24)$$

Following, for each system area or island whose security constraints have to be taken into account, an additional relaxed network flow problem is added in the optimization. For that purpose, for each dc-link additional variables indicating capacity reserved for reserve are defined, one for each system area / island under consideration. Thus in a single system area i the available reserve is equal to:

$$R_i = \mathbf{I}_{c,i} \mathbf{R} + \mathbf{I}_{dc1,i} \mathbf{T}_{dc1}^- + \mathbf{I}_{dc2,i} \mathbf{T}_{dc2}^- + \mathbf{I}_t \mathbf{R}_{t,i} \quad (4.25)$$

Where \mathbf{I}_c a vector of ones. If a generator is not located in area i then the corresponding element of vector \mathbf{I}_c is zero. The vectors \mathbf{I}_{dc1} and \mathbf{I}_{dc2} are similarly defined. For an element to be one, the corresponding dc-links power has to be transferred out of the area. Finally \mathbf{I}_t includes only those dc-links with a connecting point in area i . The vector $\mathbf{R}_{t,i}$ corresponds to the capacity reserved for reserve transfer for each dc-link with respect to area i . It should be noted that as a result of the optimization process the term $\mathbf{I}_t \mathbf{R}_{t,i}$ has to be positive. Also note that it is assumed that power transferred to other areas can be reduced and consequently is a part of the area reserve. As a result reserve requirements related to interconnection flows are transferred to the area on the receiving end only. The reserve exported from any area i has to be always less than the generated reserve in that area. That is:

$$\mathbf{I}_{c,i} \mathbf{R} \geq \mathbf{I}_t \mathbf{R}_{t,i} \quad (4.26)$$

For the j -th dc-link the following relation has to stand:

$$T_{dc1}^{j-} + R_{t,i}^j \leq T_{dc}^{j,max}, \mathbf{0} \leq T_{dc1}^{j-} \quad (4.27)$$

The same relation applies for the other end of the dc-link. Finally additional inequality constraints have to be included to ensure that the available reserve satisfies the N-1 security criterion or a variant of it, as described in the previous section.

The analysis up until now indicates how reserve size requirement may be determined, as well as how it might be distributed among various generators. Determining reserve costs however, can be another problem by itself. Traditionally the reserve cost is the sum of two components, the costs associated with keeping the generator running at a low operating point (possibly in place of a more economic one, and not at its optimal efficiency point) and the cost of starting-up the generator (if it was not already on operation). These costs may be obtained as part of the solution of the corresponding unit commitment problem. This integer programming problem can be very computationally intensive to solve, and thus its inclusion prohibitive in planning studies. At the same time, in a restructured energy market, reserve costs will be dependent on market rules as well as the disposition of the generators. For example, as discussed in [63] if as a rule generators are paid for reserve power delivered then high bids will be offered (i.e. cost coefficients higher than those of generation) to account for the probability of the reserve not being utilized at all. On the contrary if generators are paid based on reserve allocated, then low prices may be expected. In [64] the possibility of incorporating opportunity costs payment is considered, while in [59] pay-as-bid and uniform pricing alternatives are discussed. In this work it is assumed that reserve costs may be recuperated through the marginal energy prices consumers pay. No additional fees are considered. An average reserve cost per *MW* provided is assumed for each generator based on [65], where the average cost from a newly constructed power plant on an island (Crete) is estimated equal to 147 *k€/MW/year* or approximately 16.8 *€/MWh*. This value is suitably scaled for existing units based on their type and operation costs.

4.5 Optimal Power Flow Equations Summary

The equations derived in previous sections are summarized here for the sake of clarity. In this section summation notation is used. A brief description of the variables used, in order of appearance, is also repeated here. Consequently:

$$f = \sum_{i \in \Omega_c} c_{c,i} P_{c,i} + \sum_{i \in \Omega_c} c_{r,i} R_{c,i} + \sum_{i \in \Omega_w} c_{w,i} P_{w,i} - \sum_{i \in \Omega_d} c_{d,i} P_{d,i} \quad (4.28)$$

$c_{c,i}$	Cost of the i -th conventional generator.
$c_{w,i}$	Cost of the i -th conventional generator.
$c_{d,i}$	Curtailment penalty for the i -th demand block.
$c_{r,i}$	Reserve cost of the i -th conventional generator.
$P_{c,i}$	Power output of the i -th conventional generator.
$P_{d,i}$	Power demand of the i -th load block.
$P_{w,i}$	Power output of the i -th wind park.
$R_{c,i}$	Reserve provided by the i -th conventional generator.
Ω_c	Set of all conventional generators.
Ω_d	Set of all demand blocks.
Ω_w	Set of all wind parks.

$$\sum_{i \in \Omega_c^{b,j}} P_{c,i} + \sum_{i \in \Omega_w^{b,j}} P_{w,i} - \sum_{i \in \Omega_d^{b,j}} P_{d,i} = \sum_{i \in \Omega_b^{l,j}} (T_{i,j} + \frac{1}{2} T_{l,i}) + \sum_{i \in \Omega_b^{r,j}} (T_{j,i}^- - T_{j,i}^+), j \in \Omega_b \quad (4.29)$$

$$T_{i,j} = (\delta_j - \delta_k) / y_i, i \in \Omega_l, j, k \in \Omega_b^{l,i}, j \neq k \quad (4.30)$$

$$T_{l,i} = r_i T_{i,j}^2, i \in \Omega_l \quad (4.31)$$

$$T_{j,i}^- - T_{k,i}^+ = R_{e,i} J_{dc,i}^2 = \frac{R_{e,i}}{(V_{dc,i}^{nom})^2} (T_{j,i}^-)^2 = u_i (T_{j,i}^-)^2, i \in \Omega_t, j, k \in \Omega_b^{t,i}, j \neq k \quad (4.32)$$

r_i	Resistance of ac line i .
y_i	Inductance of ac line i .
$R_{e,i}$	Equivalent dc resistance of dc-link i .
$T_{j,i}^+$	Power delivered from dc-link i to bus j .

$T_{j,i}^-$	Power absorbed from dc-link i from bus j .
$T_{i,j}$	Power transferred through ac line i from bus j .
$T_{l,i}$	Losses of ac line i .
Ω_b	Set of all system buses.
Ω_l	Set of all ac transmission lines.
Ω_t	Set of all dc interconnections.
$\Omega_b^{l,i}$	Subset of buses connected by line i .
$\Omega_b^{t,i}$	Subset of buses connected by dc-link i .
$\Omega_u^{b,i}$	Subset of u connected to bus i .

$$P_{c,i} + R_{c,i} \leq P_{c,i}^{max}, 0 \leq P_{c,i}, 0 \leq R_{c,i}, i \in \Omega_c \quad (4.33)$$

$$0 \leq P_{d,i} \leq P_{d,i}^{max}, i \in \Omega_d \quad (4.34)$$

$$0 \leq P_{w,i} \leq P_{w,i}^{max}, i \in \Omega_w \quad (4.35)$$

$$T_{i,j} \leq T_i^{max}, i \in \Omega_l \quad (4.36)$$

$$-T_i^{max} + T_{j,i}^- \leq R_{t,i}^k \leq T_i^{max} - T_{j,i}^+, i \in \Omega_t, j \in \Omega_b^{t,i}, k \in \Omega_A \quad (4.37)$$

$$0 \leq T_{j,i}^-, 0 \leq T_{j,i}^+, i \in \Omega_t, j \in \Omega_b^{t,i} \quad (4.38)$$

$R_{t,i}^k$	Transmission capacity margin for reserve of dc-link i with respect to area j .
Ω_A	Set of all system areas / islands.

$$R_j = \sum_{i \in \Omega_c^j} R_{c,i} + \sum_{i \in \Omega_l^j} T_{j,i}^- + \sum_{i \in \Omega_t^j} R_{t,i}^j, j \in \Omega_A \quad (4.39)$$

$$P_{c,i} + R_{c,i} \leq R_j, j \in \Omega_A, i \in \Omega_c^{A,j} \quad (4.40)$$

$$P_{w,i} \leq R_j, j \in \Omega_A, i \in \Omega_w^{A,j} \quad (4.41)$$

$$T_{k,i}^+ + R_{t,i}^j \leq R_j, j \in \Omega_A, i \in \Omega_t^{A,j}, k \in \Omega_b^{t,i} \cap \Omega_b^{A,j} \quad (4.42)$$

$$\sum_{i \in \Omega_t^{A,j}} R_{t,i}^j \leq \sum_{i \in \Omega_c^{A,j}} R_{c,i}, j \in \Omega_A \quad (4.43)$$

R_j	Available reserve power in area j .
$R_{t,i}^k$	Transmission capacity margin for reserve of dc-link i with respect to area j .
$\Omega_u^{A,j}$	Subset of u that belongs to area j .

The above optimization problem may be solved by any non-linear programming algorithm or, if losses components are linearized, by any linear programming method. In this work an interior point method was used.

4.6 Interior Point Optimization Algorithm

Interior point methods were originally used to solve linear problems. They are so called because unlike typical linear programming algorithms (e.g. the simplex method) that search for the optimal solution points at the boundary of the feasible set, they find the solution while moving in the interior of the that set [66]. The algorithm's use was later extended in the solution of non-linear problems, including optimal power flows [67,68,69]. The standard non-linear programming problem has the following form:

$$\min_x f(x) \quad (4.44)$$

$$h(x) = 0 \quad (4.45)$$

$$g(x) \leq 0 \quad (4.46)$$

The problem is reformulated as follows using an added logarithmic term in the objective function, called a barrier function:

$$\min_x f(x) - \gamma \sum_i \ln(s_i) \quad (4.47)$$

$$h(x) = 0 \quad (4.48)$$

$$g(x) + s = 0, s \geq 0 \quad (4.49)$$

This problem is simpler than the initial since it contains only equality constraints. As γ approaches zero, the solution approaches that of the original problem. Starting from an initial point x_0 one commonly used approach to searching for the optimal solution, is taking the so called Newton step. This involves solving the first order KKT conditions. Taking the Lagrangian function:

$$L = f + \lambda^T h(x) + \mu^T (g(x) + s) - \gamma \sum_i \ln(s_i) \quad (4.50)$$

Then the first order optimality conditions are:

$$\nabla_x L = \nabla_x f + \nabla_x h^T \lambda + \nabla_x g^T \mu = 0 \quad (4.51)$$

$$\nabla_\mu L = g^T + s^T = 0 \quad (4.52)$$

$$\nabla_\lambda L = h^T = 0 \quad (4.53)$$

$$\nabla_s L = \mu^T - \gamma e^T s^{-1} \quad (4.54)$$

where e is a vector of ones. The above equations are solved using the Newton's method, and the solution variables x, s, λ, μ are updated accordingly. Further details may be found in [70,71].

Power System Planning

5.1 Introduction

Planning in power systems essentially means expansion, either in transmission or generation. And expansion means investments. There are two main factors driving investment in a power system. The first is of course profit and the second quality of service. And both of these factors are solely dependent on power demand. Along these lines, the following sections focus on the identification of optimal expansion approaches in a power system, through the definition of suitable indices and introduction of appropriate optimization methods.

5.2 Investment Evaluation Criteria

The target of an index in the power system planning case should be to show either the degree to which an investment is beneficial to the investor, or the degree to which an investment is necessary for quality of supply reasons. The first case has to do mostly with the economic viability of the investment, the second with system reliability. Indices considered representative for each case will be presented in the following sections.

5.2.1 Economic Evaluation

The power system analysis methods presented in previous chapters provide the basis for the evaluation of any economic quantity. A question arises however as to how the investor is paid back for his investment. The answer, especially when transmission is concerned, depends largely on the legislation of each different country and the procedures followed by the local system operator. In order to bypass this however, and with a market environment in mind, the change in overall social welfare is a good indicator of whether or not an investment is worthwhile. This may be defined as the sum of producers and consumers surplus. Thus its improvement implies that profit may be made. And if this profit is more than enough to cover the costs, then the investment is worthwhile.

In this work it is assumed that the demand is largely inelastic. As a result, social welfare maximization is equivalent with cost minimization in the system [72]. This is also in line within the optimal power flow optimization cost function described by (4.7). Furthermore it is assumed that the consumer energy cost is equal to the marginal cost of the corresponding bus in the system. Consequently the consumer cost, as derived from a single load flow solution, may be defined as:

$$CC = \sum_{i=1}^{n_d} \lambda_i P_{d,i} \quad (5.1)$$

where λ_i the marginal energy cost on the bus where the demand block i is connected. This marginal energy cost is equal to the shadow price (or Lagrange coefficient) corresponding to the power balance equation of that bus. The average consumer cost on an annual basis, as derived from a n samples Monte Carlo simulation, is given by:

$$CCa = \frac{8760}{n} \sum_{i=1}^n CC_i \quad (5.2)$$

It should be noted that the marginal system cost in cases where load curtailments are required will be very high. These cases are not taken into account in the averaging in (5.2), assuming that their probability is low and thus do not have a defining role in costs estimation. These cases will be treated

separately as part of the reliability evaluation of the system. The annual consumer benefit or loss that results from an investment may be given by:

$$CBa = CCa - CCa_0 \quad (5.3)$$

where CCa_0 is the consumer cost absent the investment. In cases of multiple investments within the same year, then CCa is the combined consumer cost after all respective projects are constructed.

In order to give a complete economic evaluation the overall gains during the economic life time of the investment have to be estimated. Essentially this requires the estimation of the net present value of the project. This is one of the most widely accepted methods of investment evaluation [73]. Other approaches (for example rate of return base methods) may yield slightly different results as analyzed in [74], however they will not be further discussed here. The net present value may be defined as:

$$NPV = -IC + \sum_{i=1}^t \frac{CBa_i}{(1+r)^i} \quad (5.4)$$

where r is the rate of return, t the economic life time in years and IC the investment cost. It should be noted that t does not indicate the real life time of the investment, but rather a period during which the investor is interested in the economic assessment of that investment.

5.2.2 Reliability Evaluation

A large variety of indices are have been presented in the relevant literature as far as reliability is concerned. Some of the most commonly used are the expected energy not supplied (EENS) loss of load expectation (LOLE) and loss of load frequency (LOLF). It should be noted that the non-sequential approach adopted in this work does not allow the estimation of frequency indices. Security considerations involved in the optimal power flow formulation cover to some extent system reliability aspects and will result in a direct improvement of the above mentioned indices. However in cases where either the generating sources or transmission capacity won't be adequate, or the OPF security constraints cannot be maintained, there will be load curtailments. This cases will generally be rare but might significantly contribute to the final reliability indices values. However, due to their small probability of occurrence, it will take significantly longer for the Monte-Carlo simulation to converge. In addition, in this case also, there is the question of what should be the maximum allowable values for the various reliability indices.

Typically accepted values for reliability indices (such as 1 day in 10 years for LOLE) are not necessarily the best option for different power systems. This is argued in [75] where various reliability criteria are discussed. In the end a cost / benefit analysis is recommended. Once again a main issue is the involved computational burden. In this work it is suggested to estimate the economically optimal solution independently of any reliability considerations, and then check whether or not that solution covers reliability requirements. Quite often due to the small size of the systems involved and the nature of security constraints added to the OPF, these are often already fulfilled, or related issues may be easily identified and corrected.

5.2.3 Investment Costs

Detailed and up to date costs for the various investments are not generally easy to come by. Some typical values were considered in this work, scaled up to account for inflation and possible cost overruns. For the dc interconnection the assumed cost, based on [76], is:

$$IC = (32 \cdot 10^4 \text{ €/MW}) \cdot T_{IC}^{max} + (90 \cdot 10^4 \text{ €/km}) \cdot L_{IC} \quad (5.5)$$

Maintenance and operation costs are assumed to be equal to 3% of the installation cost. Costs for ac transmission lines are as follows, based on [34] where the detailed line parameters may also be found:

$$IC = \begin{cases} 57 \cdot 10^3 \text{ €/km} & \text{if E/150} \\ 70 \cdot 10^3 \text{ €/km} & \text{if B/150} \\ 95 \cdot 10^3 \text{ €/km} & \text{if 2B/150} \end{cases} \quad (5.6)$$

Note that only 150 kV lines were considered. The symbols E and B designate the type of conductor used (cross-section of 170 mm² and 322 mm² respectively). The symbol 2B indicates a double line.

5.3 Short Term (Static) Problem

Typically system planning is about the determination of the optimal expansion plan for a certain number of years. For each of those years the peak system load will be different, and thus system costs and investment requirements will change. Evaluation of the optimal plan for each year, irrespectively of the others, is referred to as static planning [77]. Even when limiting the problem parameters however it is still difficult to find a solution. Traditional power system planning focuses on finding the least cost plan which covers power demand while fulfilling the required reliability criteria [78]. In a deregulated power system when making an investment decision the economic aspects weigh much more. And that from a revenue maximization, rather than a cost minimization point of view. In this case market prices rather than production costs are the defining factor. Strategic bidding of market participants is what differentiates these two, and may be of significant importance [79]. Uncertainties and risks related for example to the accuracy of demand forecasts or possible withdrawal of generating resources play their own part. As a result any applied method should be capable of incorporating the relevant considerations.

As already mentioned an investment will either be economic driven or reliability driven. Focusing on economic driven investments means focusing on system marginal prices. New generation might be installed if its marginal generation cost is sufficiently lower than the system marginal energy price. Similarly new transmission might be beneficial if a sufficiently large difference exists between the marginal prices of two buses. Each investment is bound to affect system operation and might generate the need for further investments. Theoretically investments will stop once the system has a relatively flat price profile. Furthermore it might make sense to determine that investment combination which renders further investments economically non viable, while maximizing overall benefits. In this way the system operator may direct investments towards that direction.

The Monte-Carlo process described in the previous chapters may be considered as a function $Y = f(u)$, $u \in U$, where U is the discrete set of all possible investment combinations and Y the expected system costs. It should be obvious that the derivatives of this function cannot be found analytically. Therefore there are two possibilities of finding a solution to an optimization problem based on this equation: enumeration and randomized search. The process suggested in this work falls into the former category, and as is illustrated in Fig. 5.1 involves the following steps:

1. Evaluate the base (no investments) system.
2. Determine investment candidates. Each such candidate results in a new investment scenario.
3. Evaluate each investment scenario (adding the minimum possible capacity).
4. Determine new investment candidates for each investment scenario.
5. Go to step 3 and repeat the above process until no further investment candidates can be found.

It is assumed that a list of all transmission paths, where investments of any type are possible, is known beforehand. Candidate investments are selected from that list. The main issue here is finding a way to determine these candidates. Given that the target is to study the interconnection of isolated systems, it is assumed that investments in conventional generation are not allowed. An obvious quantity that indicates the need for additional transmission is the marginal cost difference between two buses. Thus investments in transmission between buses with cost difference higher than an arbitrarily selected value could be selected as candidates. By setting that value too high however, investment scenarios that could be optimal will be ignored, while by setting it too low, a very large number of investment combinations will have to be evaluated. This approach is used in [4]. Consequently, and since candidate investments generally deal with transmission paths with high losses or high congestion, in this work the following simplifying assumptions are made:

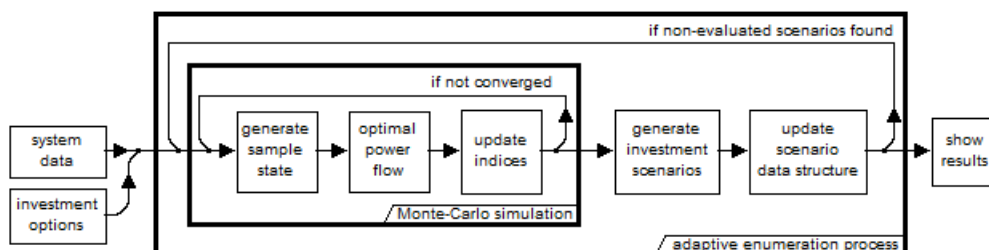


Fig. 5.1. Indicative flow diagram of the proposed method.

- Losses-driven investments will not significantly affect congestion-driven investments.
- The need for losses-driven investments may be investigated after congestion-driven investments and yield similar results as if these were optimized simultaneously.

Consequently an important quantity is the congestion probability p_g , defined equal to the percentage of time that a transmission path is loaded over 95% of its full capacity. If p_g is higher than an arbitrarily selected margin this route is assumed to be eligible for investment. Note that if the probability of congestion has a very small value it might converge much later than the marginal system cost. This however is considered acceptable. For transmission paths without a connecting line $p_g = 100\%$. It should be noted however that the smaller the marginal cost differences, the more impact losses have. Thus, when interconnecting systems with very small price differences then these assumptions might not hold. Summing up the above the following two factors determine potential investment candidate routes:

- Congestion probability higher than 1%.
- Marginal cost difference higher than that of any two buses connected by an uncongested line.

These ensure a congestion driven investment scheme. By altering these factors more general planning approaches are possible (i.e. addition of reliability indices to ensure adequacy, addition of losses costs related indices to investigate related schemes).

5.4 Indicative Results

In this section an example is setup to illustrate the presented adaptive enumeration method, which was fully implemented in Matlab. Base system data and relevant assumptions are presented, and the method's results are explained.

5.4.1 Test System

The system used in this example approximates that of the Greek island of Crete and may be seen on Fig. 5.2. It is a 16 bus system with 809 MW peak load. The base system data may be found in the tables I to III. Average conventional generator operation costs are assumed to be 64 €/MWh, 100 €/MWh, 155 €/MWh and 180 €/MWh for diesel, steam, combined cycle and gas generators respectively. These quantities were scaled for various units depending on their power output capability. Forced outage rates were set on the order of 0.2-0.5 both for conventional generators and wind parks. The system yields an average marginal cost of 138 €/MWh. The mainland grid is modeled as a single bus, and it is assumed that demand in Crete has no effect on the energy prices on the mainland. The corresponding marginal cost is 90 €/MWh. Correlation coefficients between various park wind speeds was arbitrarily set, taking into account their geographical distance. Demand was assumed constant for the duration of the study. Furthermore, it is assumed that no investments in generation take place. Two potential dc-interconnection routes were considered and their rating is assumed to take discrete values, multiples of 100 MW. In addition upgrades were considered possible for all ac transmission lines on the island.

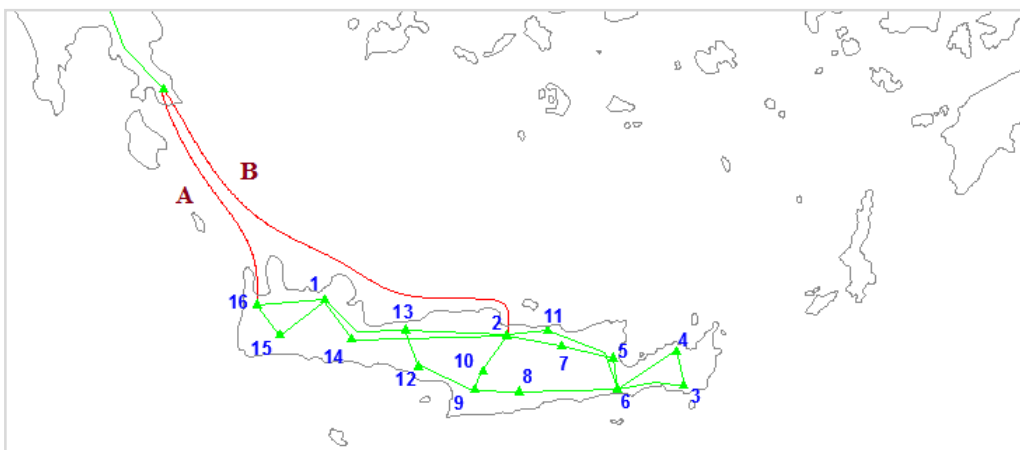


Fig. 5.2. Test System

5.4.2 Interconnection Effects Assessment

Before moving to the application of the proposed method, a simpler example is setup to illustrate the effects of the two systems interconnection and the effects of reserve related constraints in the optimal power flow problem. In the examples described in this section for simplicity losses are ignored. Furthermore only a single interconnection is considered and no investments are allowed in the ac transmission system. Solutions are examined with and without reserve constraints in the optimal power flow formulation.

Given the large marginal energy cost difference between the two systems, a new interconnection allows the transfer of cheap energy to the island system. This effectively leads to the shut-down of the more expensive generating units, which results in lower marginal energy cost for the island. This is depicted in Fig. 5.3. As the interconnection capacity (in route B) increases, so does the marginal cost decrease until the energy costs of the two systems become equal. Given that it was assumed that the demand in Crete has no effect on the marginal cost of the mainland grid, then the energy price may become as low as 90 €/MWh. However, when reserve requirements are taken into account the resulting price is higher. The reason is that as the interconnection typically provides much more energy than any local generating unit, for every MW provided through it an extra cost is incurred to provide the additional required reserve.

While increased interconnection capacity results in lower energy prices, that does not mean that it is always beneficial to pursue the minimum possible price. This is directly depicted in the diagrams of Fig. 5.4. An interconnection capacity increase beyond 350 MW in route A yields diminishing returns. The reason is that the ac transmission system on the island cannot transfer more energy from the west to

TABLE I
TRANSMISSION SYSTEM DATA

from	to	type									
1	13	B/150	2	11	B/150	6	11	B/150	8	9	B/150
1	14	B/150	2	13	B/150	4	6	E/150	9	10	E/150
1	15	B/150	2	14	B/150	5	6	B/150	9	12	B/150
1	16	B/150	3	4	B/150	5	7	B/150	12	13	B/150
2	7	B/150	3	6	B/150	6	8	B/150	15	16	B/150
2	10	E/150	3	6	B/150	6	9	B/150			

TABLE II
DEMAND DATA

bus	peak (MW)						
1	155	6	25	11	92	16	20
2	114	7	78	12	24	17	10
3	18	8	17	13	84		
4	20	9	47	14	28		
5	56	10	15	15	16		

TABLE III
CONVENTIONAL & RENEWABLE GENERATION DATA

bus	type	max. (MW)	num.	bus	type	max. (MW)	num.
2	steam	16	2	1	gas	46	2
2	steam	26	3	1	cc	45	1
2	gas	51	1	4	wind	56	1
2	gas	14	1	4	wind	33	1
2	gas	19	2	5	wind	12	1
2	gas	38	1	9	wind	18	1
2	diesel	24	4	10	wind	15	1
3	diesel	51	4	2	wind	10	1
3	steam	50	2	13	wind	10	1
1	gas	60	2	1	wind	11	1
1	gas	38	1	16	wind	19	1

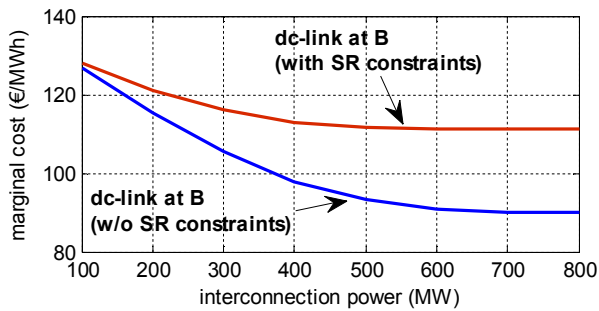


Fig. 5.3. Marginal energy cost as a function of interconnection capacity.

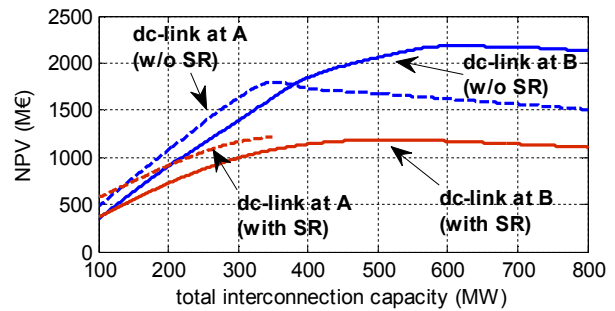


Fig. 5.4. Net present value as a function of interconnection capacity for the two different routes.

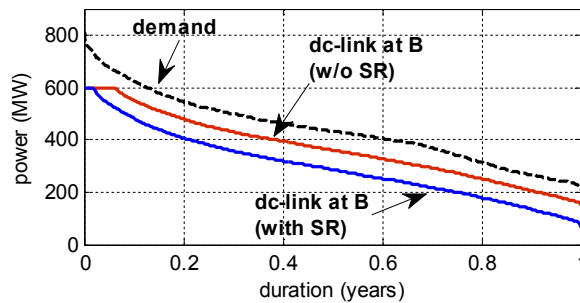


Fig. 5.5. Interconnection utilization duration curve for a 600 MW dc-link.

the east side of the island. Additional investments would be required. While similar restrictions do not exist for a dc-link in route B, it may be seen that an interconnection higher than 550 MW also does not offer any significant improvement in the net present value, as the additional investment cost outweighs the benefits derived from the resulting energy cost reduction. In the same figure the reduced benefits when reserve constraints are included should also be noted. This observation underlines the importance of such factors in the evaluation of the optimal interconnection size. This is also clearly indicated in Fig. 5.5 where the impact of reserve may be seen in the utilization of the interconnection. Without considering reserve the dc-link covers nearly all energy demand minus that generated by renewable sources. When reserve is taken into account however the interconnection is not fully utilized for energy transfer. It is often used to provide reserve to the island, while a few low cost units are also in operation.

5.4.3 Adaptive Enumeration Method Results

The method's application results in a tree like structure as shown on Fig. 5.6. Each node represents a possible investment scenario. The number next to each node is the ratio of that scenario's benefit to the maximum achievable benefit. In order to better illustrate how the method works let us consider three separate points. At point A no investments have been made. No congestion issues have been found to exist in the island system itself. However due to the large marginal cost difference between the island and the mainland system the two sea routes are considered to be eligible for investment. So two subsequent scenarios come up, with a 100 MW interconnection at route A and B respectively. The added transmission capacity should allow the transfer of energy from the low energy price mainland grid to the high price island. If adequate power is transferred then the highest cost generator will be displaced, reducing the marginal energy cost, which in turn results in benefit for the consumers. Point B corresponds to a scenario of a 500 MW interconnection in A, and a 100 MW interconnection in B. Due to congestion in the lines transferring power for the west to the east of the island the interconnection in A is not fully utilized. Two investment scenarios come up, one corresponding to an increased capacity interconnection in B, and one corresponding to an additional investment in the ac transmission of the island. Finally point C is the best solution found with two equally sized interconnections at about 700 MW and an upgrade at a specific ac line on the western part of the island system to 404 MW. The end nodes correspond to cases where there is no need for further investment as indicated by the selected probabilistic criteria. The investment costs of generated scenarios may be easily compared, as well as the loss of benefit associated with following investment plans other than the optimal.

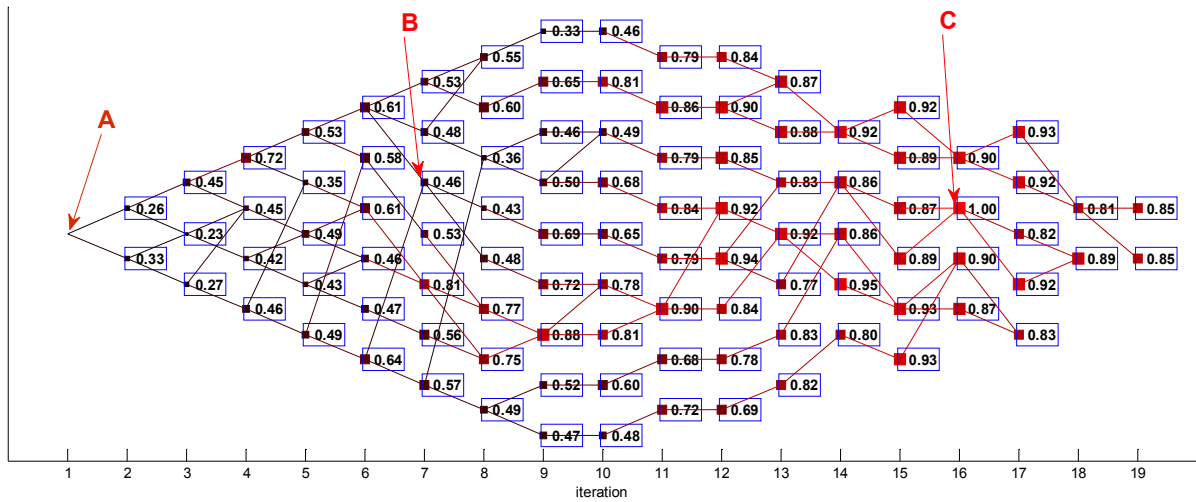


Fig. 5.6. Derived decision tree.

5.5 Long Term (Dynamic) Problem

The previous solution focused on a specific system state, i.e. a given demand distribution and given generating sources. Over the years covered by the planning process several changes might take place. Power consumption might increase or decrease, generation or transmission expansions might have been programmed which will cover part of the period under study. Furthermore a change on the rules governing the energy market operation might be in order. And quite often all these factors may have a degree of uncertainty associated with them. The problem can become even more complex, if the possibility of delaying a potential investment were to be considered. A simple approach to include changes in the system during the planning period, would be to break the latter down to smaller periods during which the system remains unchanged. A Monte Carlo simulation would have to be separately run for each of those periods and the resulting benefits would have to be combined. As can be expected the computational cost might be significantly increased but the whole process could be effectively optimized. This however is outside the scope of this work.

Conclusions

6.1 Conclusions

A method for the determination of an optimal transmission expansion plan in a power system has been presented in this work. The method generates a map of all possible transmission expansion scenarios, based on the assumption that the needs and drives for potential investments may be described through suitable probabilistic indices. Both the optimal scenario and the one that will be finally realized based on the capital holders' decisions are included in that map. A key idea is that the system operator may promote, possibly through various economic incentives, the solutions which are close to the optimal. While the method can be generally applied in any system and may also include investments in generation, emphasis has been given in cases of interconnection of isolated systems with dc-links. Simplified models for the dc interconnections were derived and particular attention was given on security constraints related to operating reserve. Losses over the interconnection can play an important role in its usage thus they have to be adequately modeled. Furthermore reserve constraints may have a significant impact on both interconnection usage and the final system marginal costs. As a result the final benefits from the interconnection may be significantly affected. Consequently this also is an important factor that has to be considered. A potential electrical interconnection of Crete with mainland Greece was used as an example to demonstrate the method's application.

6.2 Future Work

The presented method is generally applicable in the transmission and / or generation expansion of any power system, and can generate a map that includes all possible expansion plans of interest. Improvements however are possible in three basic areas: system costs estimation, investments determination and plan selection. As far as costs estimation is concerned a different formulation might be desirable that allows for a more general social benefit optimization (including both consumers, generation companies, and perhaps transmission rights holders). Also the inclusion of additional security constraints might be warranted. Furthermore an extra module could be incorporated to the method, to allow the determination and inclusion only of the most important transmission constraints (i.e. those which actually impose limits on system operation), and thus reduce the computational burden of the method. The criteria (indices) used to determine candidate investments, may also be an area for additional research. While a large variety of probabilistic indices have been proposed in existing literature not all may be translated either to system reliability or to monetary value. Selection of a suitable general set of indices and complementing the method with a module to determine automatically their reference values could improve the generated results. Last but not least, an issue of interest would be to determine the best solution under presence of various uncertainties. While possible planning scenarios could be generated with the method, an extension would be required (based on decision theory) to select one among them.

References

- [1] C.-K. Kim, V. K. Sood, G.-S. Jang, S.-J. Lim, and S.-J. Lee, *HVDC Transmission: Power Conversion Applications in Power Systems*. Wiley, 2009.
- [2] G. Latorre, R. D. Cruz, J. M. Areiza, and A. Villegas, "Classification of Publications and Models on Transmission Expansion Planning," *IEEE Trans. Power Systems*, vol. 18, no. 2, pp. 938-946, May 2003.
- [3] J. Choi, et al., "A Method for Transmission System Expansion Planning Considering Probabilistic Reliability Criteria," *IEEE Trans. Power Systems*, vol. 20, no. 3, pp. 1606-1615, Aug. 2005.
- [4] M. O. Buygi, G. Balzer, H. M. Shanechi, and M. Shahidehpour, "Market-Based Transmission Expansion Planning," *IEEE Trans. Power Systems*, vol. 19, no. 4, pp. 2060-2067, Nov. 2004.
- [5] M. S. Sepasian, A. A. Foroud, and A. R. Hatami, "A Multiyear Security Constrained Hybrid Generation-Transmission Expansion Planning Algorithm Including Fuel Supply Costs," *IEEE Trans. Power Systems*, vol. 24, no. 3, pp. 1609-1618, Aug. 2009.
- [6] A. K. Kazerooni and J. Mutale, "Transmission Network Planning Under Security and Environmental Constraints," *IEEE Trans. Power Systems*, vol. 25, no. 2, pp. 1169-1178, May 2010.
- [7] M. Carrion, J. M. Arroyo, and N. Alguacil, "Vulnerability-Constrained Transmission Expansion Planning: A Stochastic Approach," *IEEE Trans. Power Systems*, vol. 22, no. 4, pp. 1436-1445, Nov. 2007.
- [8] J. M. Arroyo, N. Alguacil, and M. Carrion, "A Risk-Based Approach for Transmission Network Expansion Planning Under Deliberate Outages," *IEEE Trans. Power Systems*, vol. 25, no. 3, pp. 1759-1766, Aug. 2010.
- [9] J. Choi, T. D. Mount, and R. J. Thomas, "Transmission Expansion Planning Using Contingency Criteria," *IEEE Trans. Power Systems*, vol. 22, no. 4, pp. 2249-2261, Nov. 2007.
- [10] G. B. Shrestha and P. A. J. Fonseca, "Congestion-Driven Transmission Expansion in Competitive Power Markets," *IEEE Trans. on Power Systems*, vol. 19, no. 3, pp. 1658-1665, Aug. 2004.
- [11] J. H. Zhao, Z. Y. Dong, and K. P. Wong, "Flexible Transmission Network Planning Considering Distributed Generation Impacts," *IEEE Trans. Power Systems*, vol. 26, no. 3, pp. 1434-1443, Aug. 2011.
- [12] P. Maghouli, S. H. Hosseini, M. O. Buygi, and M. Shahidehpour, "A Scenario-Based Multi-Objective Model for Multi-Stage Transmission Expansion Planning," *IEEE Trans. Power Systems*, vol. 26, no. 1, pp. 470-478, Feb. 2011.
- [13] J. H. Roh, M. Shahidehpour, and L. Wu, "Market-Based Generation and Transmission Planning With Uncertainties," *IEEE Trans. Power Systems*, vol. 24, no. 3, pp. 1587-1598, Aug. 2009.

- [14] V. K. Sood, *HVDC and Facts Controllers: Applications of Static Converters in Power Systems*. Kluwer Academic Publishers, 2004.
- [15] P. Kundur, *Power System Stability and Control*. McGraw-Hill, 1994.
- [16] J. Arrillaga, Y. H. Liu, and N. R. Watson, *Flexible Power Transmission: The HVDC Option*. Wiley, 2007.
- [17] J. Holz, "Pulsewidth Modulation for Electronic Power Conversion," *IEEE Proceedings*, vol. 82, no. 8, pp. 1194-1214, Aug. 1994.
- [18] N. Mohan, T. Undeland, and W. Robbins, *Power Electronics: Converters, Applications and Design*. Wiley, 1995.
- [19] L. Zhang, L. Harnefors, and H.-P. Nee, "Interconnection of Two Very Weak AC Systems by VSC-HVDC Links Using Power Synchronization Control," *IEEE Trans. Power Systems*, vol. 26, no. 1, pp. 344-355, Feb. 2011.
- [20] L. Zhang, L. Harnefors, and H.-P. Nee, "Modeling and Control of VSC-HVDC Links Connected to Island Systems," *IEEE Trans. Power Systems*, vol. 26, no. 2, pp. 783-793, May 2011.
- [21] T. Worzyk, *Submarine Power Cables*. Springer, 2009.
- [22] G. J. Anders, *Rating of Electrical Power Cables*. McGraw Hill, 1997.
- [23] C. L. Wadhwa, *High Voltage Engineering*. New Age International Publishers, 2007.
- [24] G. J. Anders, M. Vainberg, D. J. Horrocks, S. M. Foty, and J. Motlis, "Parameters Affecting Economic Selection of Cable Sizes," *IEEE Transactions on Power Delivery*, vol. 8, no. 4, pp. 1661-1667, Oct. 1993.
- [25] ABB, "Technical Description of HVDC Light Technology," 2008.
- [26] R. Billinton and W. Li, *Reliability Assessment of Electric Power Systems Using Monte Carlo Methods*. Plenum Press, 1994.
- [27] D. P. Kroese, T. Taimre, and Z. I. Botev, *Handbook of Monte Carlo Methods*. Wiley, 2011.
- [28] J. L. Myers and A. D. Wells, *Research Design and Statistical Analysis*. Lawrence Erlbaum, 2003.
- [29] H. Hotelling and M. R. Pabst, "Rank Correlation and Tests of Significance Involving No Assumption of Normality," *Annals of Mathematical Statistics*, vol. 7, no. 1, pp. 29-43, 1936.
- [30] N. B. Negra, O. Holmstrom, B. B. Jensen, and P. Sorensen, "Aspects of Relevance on Offshore Wind Farm Reliability Assessment," *IEEE Trans. Energy Conversion*, vol. 22, no. 1, pp. 159-166, Mar. 2007.
- [31] P. Giorsetto and K. F. Utsurogi, "Development of a New Procedure for Reliability Modeling of Wind Turbine Generators," *IEEE Trans. Power Apparatus and Systems*, vol. 102, no. 1, pp. 134-143, Jan. 1983.
- [32] B. P. Hayes, I. S. I. -A. Porpodas, S. Z. Djokic, and G. Chicco, "Equivalent Power Curve Model of a Wind Farm Based on Field Measurement Data," in *IEEE PowerTech*, Trondheim, Norway, 2011.
- [33] R. Billinton and Y. Gao, "Multistate Wind Energy Conversion System Models for Adequacy Assessment of Generating Systems Incorporating Wind Energy," *IEEE Trans. Energy Conversion*, vol. 23, no. 1, pp. 163-170, Mar. 2008.

- [34] Public Power Corporation, "Distribution Grids Planning Guide," 1995.
- [35] Berdal Strome, "Reliability, Availability and Maintainability Study Norned HVDC Cable Project," 1998.
- [36] M. Nakamura, N. Nanayakkara, H. Hatazaki, and K. Tsuji, "Reliability Analysis of Submarine Power Cables and Determination of External Mechanical Protections," *IEEE Trans. Power Delivery*, vol. 7, no. 2, pp. 895-902, Apr. 1992.
- [37] N. Alguacil, A. L. Motto, and A. J. Conejo, "Transmission Expansion Planning: A Mixed-Integer LP Approach," *IEEE Trans. Power Systems*, vol. 18, no. 3, pp. 1070-1077, Aug. 2003.
- [38] Y.-C. Chang, W.-T. Yang, and C.-C. Liu, "A New Method for Calculating Loss Coefficients," *IEEE Trans. Power Systems*, vol. 9, no. 3, pp. 1665-1671, Aug. 1994.
- [39] S. d. I. Torre, A. J. Conejo, and J. Contreras, "Transmission Expansion Planning in Electricity Markets," *IEEE Trans. Power Systems*, vol. 23, no. 1, pp. 238-248, Feb. 2008.
- [40] A. Sharifnia and H. Z. Aashtiani, "Transmission Network Planning: A Method for Synthesis of Minimum Cost Secure Networks," *IEEE Trans. Power Systems*, vol. 104, no. 8, pp. 2026-2034, Aug. 1985.
- [41] A. S. D. Braga and S. J. T., "A Multiyear Dynamic Approach for Transmission Expansion Planning and Long-Term Marginal Costs Computation," *IEEE Trans. Power Systems*, vol. 20, no. 3, pp. 1631-1639, Aug. 2005.
- [42] H. Ambriz-Perez, E. Acha, and C. R. Fuerte-Esquivel, "High Voltage Direct Current Modelling in Optimal Power Flows," *International Journal of Electrical Power & Energy Systems*, vol. 30, no. 3, pp. 157-168, Mar. 2008.
- [43] A. Pizano-Martinez, C. R. Fuerte-Esquivel, H. Ambriz-Perez, and E. Acha, "Modeling of VSC-Based HVDC Systems for a Newton-Raphson OPF Algorithm," *IEEE Trans. Power Systems*, vol. 22, no. 4, pp. 1794-1803, Nov. 2007.
- [44] A. Lotfjou, M. Shahidehpour, Y. Fu, and Z. Li, "Security Constrained Unit Commitment With AC/DC Transmission Systems," *IEEE Trans. Power Systems*, vol. 25, no. 1, pp. 531-542, Feb. 2010.
- [45] V. Miranda, J. N. Fidalgo, J. A. P. Lopes, and L. B. Almeida, "Real Time Preventive Actions for Transient Stability Enhancement with a Hybrid Neural Network Optimization Approach," *IEEE Trans. Power Systems*, vol. 10, no. 2, pp. 1029-1035, May 1995.
- [46] D. Gan, R. J. Thomas, and R. D. Zimmerman, "Stability Constrained Optimal Power Flow," *IEEE Trans. Power Systems*, vol. 15, no. 2, pp. 535-540, May 2000.
- [47] A. P. Martinez, C. R. F. Esquivel, and D. R. Vega, "A New Practical Approach to Transient Stability Constrained Unit Commitment," *IEEE Trans. Power Systems*, vol. 26, no. 3, pp. 1686-1696, Aug. 2011.
- [48] Z. Zhu, *Optimization of Power System Operation*. Wiley, 2009.
- [49] E. J. Thalassinakis and E. N. Dialynas, "A Monte Carlo Simulation Method for Setting the Underfrequency Load Shedding Relays and Selecting the Spinning Reserve Policy in Autonomous Power Systems," *IEEE Trans. Power Systems*, vol. 19, no. 4, pp. 2044-2052, Nov. 2004.
- [50] E. Loukarakis and G. Stavrakakis, "Investigation of Spinning Reserve Impact on Isolated Systems DC Interconnection Feasibility," in *IEEE International Conference on Environment and Electrical Engineering*,

Rome, Italy, 2011.

- [51] L. T. Anstine, et al., "Application of Probability Methods to the Determination of Spinning Reserve Requirements for the Pennsylvania - New Jersey - Maryland Interconnection," *IEEE Trans. Power Apparatus and Systems*, vol. 82, no. 68, pp. 726-735, 1963.
- [52] R. Moreno, D. Pudjianto, and G. Strbac, "Future Transmission Network Operation and Design Standards to Support a Low Carbon Electricity System," in *IEEE Power and Energy Society General Meeting*, Minneapolis, 2010.
- [53] R. Billinton and R. N. Allan, *Reliability Evaluation of Power Systems*. Plenum Press, 1996.
- [54] M. A. Ortega-Vazquez and D. S. Kirschen, "Optimizing the Spinning Reserve Requirements Using a Cost / Benefit Analysis," *IEEE Trans. Power Systems*, vol. 22, no. 1, pp. 24-33, Sep. 2007.
- [55] M. A. Ortega-Vasquez and D. S. Kirschen, "Estimating the Spinning Reserve Requirements in Systems with Significant Wind Power Penetration," *IEEE Trans. Power Systems*, vol. 24, no. 1, pp. 114-124, Feb. 2009.
- [56] L. L. Garver, "Effective Load Carrying Capability of Generating Units," *IEEE Trans. Power Apparatus and Systems*, vol. 85, no. 8, pp. 910-919, Aug. 1996.
- [57] D. Chattopadhyay and R. Baldnick, "Unit Commitment with Probabilistic Reserve," in *IEEE Power Engineering Society Winter Meeting*, 2002.
- [58] M. Flynn, W. P. Sheridan, J. D. Dilon, and M. J. O'Malley, "Reliability and Reserve in Competitive Electricity Market Scheduling," *IEEE Trans. Power Systems*, vol. 16, no. 1, pp. 78-87, Feb. 2001.
- [59] J. Wang, X. Wang, and Y. Wu, "Operating Reserve Model in the Power Market," *IEEE Trans. Power Systems*, vol. 20, no. 1, pp. 223-229, Feb. 2005.
- [60] H. B. Gooi, D. P. Mendes, K. R. W. Bell, and D. S. Kirschen, "Optimal Scheduling of Spinning Reserve," *IEEE Trans. Power Systems*, vol. 14, no. 4, pp. 1485-1492, Nov. 1999.
- [61] J. W. O'Sullivan and M. J. O'Malley, "A New Methodology for the Provision of Reserve in an Isolated Power System," *IEEE Trans. Power Systems*, vol. 14, no. 2, pp. 519-524, May 1999.
- [62] R. Doherty, G. Lallor, and M. O'Malley, "Frequency Control in Competitive Electricity Market Dispatch," *IEEE Trans. Power Systems*, vol. 20, no. 3, pp. 1588-1596, Aug. 2005.
- [63] E. H. Alen and M. D. Ilic, "Reserve Markets for Power Systems Reliability," *IEEE Trans. Power Systems*, vol. 15, no. 1, pp. 228-233, Feb. 2000.
- [64] D. Gan and E. Litvinov, "Energy and Reserve Market Designs With Explicit Consideration to Lost Opportunity Costs," *IEEE Trans. Power Systems*, vol. 18, no. 1, pp. 53-59, Feb. 2003.
- [65] Greek Regulatory Authority for Energy, "Decision no.1333," 2010.
- [66] D. Bertsimas and J. N. Tsitsiklis, *Introduction to Linear Optimization*. Athena Scientific, 1997.
- [67] H. Wang, C. E. Murillo-Sanchez, R. D. Zimmerman, and R. J. Thomas, "On Computational Issues of Market-Based Optimal Power Flow," *IEEE Trans. Power Systems*, vol. 22, no. 3, pp. 1185-1193, Aug. 2007.

- [68] A. A. Sousa, G. L. Torres, and C. A. Canizares, "Robust Optimal Power Flow Solution Using Trust Region and Interior-Point Methods," *IEEE Trans. Power Systems*, vol. 26, no. 2, pp. 487-499, May 2011.
- [69] R. D. Zimmerman, C. E. Murillo-Sanchez, and R. J. Thomas, "MATPOWER: Steady-State Operations, Planning, and Analysis Tools for Power Systems Research and Education," *IEEE Trans. Power Systems*, vol. 25, no. 4, Jun. 2010.
- [70] S. J. Wright, *Primal-Dual Interior-Point Methods*. Society for Industrial and Applied Mathematics, 1997.
- [71] R. H. Byrd, M. E. Hribar, and J. Nocedal, "An Interior Point Algorithm for Large Scale Nonlinear Programming," *SIAM Journal on Optimization*, vol. 9, pp. 877-900, 1997.
- [72] D. S. Kirschen and G. Strbak, *Fundamentals of Power Systems Economics*. Wiley, 2004.
- [73] G. Rothwell and T. Gomez, *Electricity Economics: Regulation and Deregulation*. Wiley, 2003.
- [74] E. Loukarakis, K. Kalaitzakis, E. Koutroulis, and G. Stavrakakis, "Investment Perspectives on the Interconnection of Isolated Systems with the Mainland Grid," in *IASTED European Conference on Power and Energy Systems*, Crete, Greece, 2011.
- [75] D. Camac, R. Bastidas, R. Nadira, C. Dortolina, and H. M. Merrill, "Transmission Planning Criteria and Their Application Under Uncertainty," *IEEE Trans. Power Systems*, vol. 25, no. 4, pp. 1996-2003, Nov. 2010.
- [76] D. N. Newbery, N. H. Von der Fehr, and E. Van Damme, "UK-Netherlands DC Interconnector," report of Market Surveillance Committee of DTe, 2003.
- [77] H. Seifi and M. S. Sepacian, *Electric Power System Planning*. Springer, 2011.
- [78] F. F. Wu, F. S. Zheng, and F. S. Wen, "Transmission Investment and Expansion Planning in a Deregulated Electricity Market," *Energy*, vol. 31, no. 7, pp. 954-966, Jun. 2006.
- [79] California ISO, "Transmission Economic Assessment Methodology," 2004.